TAMPERE UNIVERSITY OF TECHNOLOGY

JOUNI KOPSALA

INDOOR MIMO PERFORMANCE WITH HSPA+ AND LTE

Master of Science Thesis

Supervisor: M.Sc Jarkko Itkonen
Examiner: Prof. Jukka Lempiäinen
Examiner and topic approved in the
Faculty of Computing and Electrical
Engineering Council meeting on
9 November 2011

ABSTRACT

TAMPERE UNIVERSITY OF TECHNOLOGY
Master's Degree Programme in Information Technology
KOPSALA, JOUNI: Indoor MIMO performance with HSPA+ and LTE
Master of Science Thesis, 64 pages, 7 Appendix pages
June 2012
Major: Wireless Communication
Examiner: Professor Jukka Lempiäinen
Keywords: MIMO, HSPA+, LTE, indoor network, field measurements.

The focus of this thesis is to perform and study indoor measurements with both HSPA+ and LTE MIMO setups. The reason behind this study is to validate the benefits of MIMO implementation in indoor cells. MIMO scheme is compared against single antenna configurations and other test cases, such as different antenna diversity setups for spatial multiplexing and studying the effect of attenuation imbalance in MIMO antenna lines. In terms of performance, air interface throughput is used to compare different setups. Measurements were performed in a office building, using single cell with minimal interfernce. Throughput results were gathered in both mobile routes and in static locations, using laptop and spatial multiplexing MIMO capable commercial USB modems.

Results obtained from these measurements follow the expectations, for the most part, made in measurement plan, based on literacy and theory behind MIMO and wireless radio access methods. On good channel conditions, near the antenna and at LOS locations, the maximal practical throughput peaks can be seen, and average rate is notably higher than single antenna setups. For HSPA+ on best channel conditions, spatial multiplexing MIMO gain is around 50% compared to single antenna and in worse channel condition, the average gain is only around 5 to 15%. With LTE, the MIMO gain in good channel conditions averages around 60% and on worse channel it still gives 15 to 30% average gain.

LTE with OFDMA is more stable in terms of throughput variance than HSPA+ using WCDMA. Static measurement results show that current state of dual stream MIMO reception is very sensitive to receiver antenna orientation with both HSPA+ and LTE. Small change in receiver orientation can have a large effect to obtained throughput rate.

TIIVISTELMÄ

TAMPEREEN TEKNILLINEN YLIOPISTO
Tietotekniikan koulutusohjelma
KOPSALA, JOUNI: MIMO:n suorituskyky sisätiloissa HSPA+ ja LTE tekniikoilla
Diplomityö, 64 sivua, 7 liitesivua
Kesäkuu 2012
Pääaine: Langaton tietoliikenne
Tarkastaja: Professori Jukka Lempiäinen
Avainsanat: MIMO, HSPA+, LTE, sisäverkko, mittaukset.

Tämän diplomityön päämääränä on mitata ja analysoida HSPA+:n ja LTE:n MIMO suorituskykyä sisätilassa. Tutkimuksen tarkoitus on selvittää mahdollisia MIMO:n tuomia etuja sisäverkkojen toteutuksessa. Kahden antennin MIMO:a verratan yhden antennin toteutusta vastaan ja lisäksi tarkatellaan muita tapauksia, kuten eri keinoja toteuttaa antenni diversiteetti *spatial multiplexing* MIMO:lle ja MIMO:n antennilinjojen vaimennuksen epätasapainon vaikutusta. Suorituskykyä mitataan saavutetun ilmarajapinnan tiedonsiirtonopeuksilla eri testitapauksissa.

Mittaukset suoritettiin toimistorakennuksessa yhdellä solulla ja minimaalisella häiriöllä. Siirtonopeus mittaukset suoritettiin liikkumalla reittejä pitkin sekä paikallaan kiinteissä mittauspaikoissa. Mittalaitteina käytettiin kannettavaa tietokonetta, jossa mittaohjelmana on Nemo Outdoor. Käytetyt USB modeemit ovat kaupallisesti saatavilla ja tukevat *spatial multiplexing* MIMO ominaisuutta.

Mittauksista saadut tulokset ovat pääsääntöisesti kirjallisuudesta saatujen ja testisuunnitelmassa tehtyjen odotusten mukaisia. Hyvässä radiokanavassa saadut tulokset, lähellä tai näköyhteydessä lähteysantenniin päästiin hetkittäin hyvin lähelle käytännön maksimiarvoja. HSPA+:n *spatial multiplexing* MIMO tuo hyvällä radiokanavalla keskimäärin 50% parannuksen siirtonopeuksiin, mutta huonommissa radiokanavissa saatu hyöty jää 5 ja 15% välille. LTE:llä hyvissä olosutheissa saatu hyöty on keskimäärin 60% ja huonomissa olosuhteissa MIMO:n siirtonopeudet ovat keskimäärin 15 - 30% paremmat kuin yhdellä antennilla.

LTE:n käyttämä OFDMA tekniikka on tulosten perusteella vakaampi kuin HSPA+:n WCDMA tekniikka. Tämä näkyy siirtonopeuden vaihtelusta, sekä referenssi-signaalin voimmakuuden vaikutuksesta suorituskykyyn. Kiinteässä paikassa suoritettujen mittausten perusteella MIMO:n nykyinen vastaanotin on erittäin herkkä modeemin suuntaukselle. Pieni muutos vastaanottimen suunnassa voi näkyä merkittävänä muutoksena tiedonsiirtonopeudessa.

PREFACE

This Master of Science Thesis has been written for the completion of my M.Sc degree in Tampere University of Technology . The thesis work been done for Nokia Siemens Networks (NSN), department of Network Planning and Optimization in Karaportti, Espoo. Writing process and measurement work were carried out during Summer and Fall 2011.

I would like to thank my examiner Jukka Lempiäinen for introducing me to the work and for all the advices and guidance he provided.

Additionally, I'm very tankful to my instructor Jarkko Itkonen for the invaluable assistance and guidance for my thesis work. To Jyri Lamminmäki for his expertise and help with LTE. To Florian Reymond for giving me opportunity to work with NSN. Special thanks also to my line manager Heikki Tuohiniemi for keeping the work environment functional. And of course to all other NSN NPO employees for making NSN such a great place to work, Thank you!

Last but not the least, I would like to thank my dear wife Sheena for all the support and love I've got. Salamat mahal ko!

I would like to dedicate this thesis for my parents and family. With their constant support and encouragement, I'm able to be where I am today.

Espoo 2.12.2011

Jouni Kopsala

CONTENTS

LIST OF ABBREVIATIONS

3G	Third Generation
3GPP	3rd Generation Partnership Project
BER	Bit Error Rate
BTS	Base Transceiver Station
CSI	Channel State Information
CQI	Channel Quality Indicator
DAS	Distributed Antenna System
FDD	Frequency Division Duplex
FSL	Free-Space Loss, see also FSPL
FSPL	Free-Space Path Loss
HSDPA	High Speed Downlink Packet Access
HSPA	High Speed Packet Access
HSPA+	Evolved HSPA
IP	Internet Protocol
ISI	Inter Symbol Interference
LOS	Line-of-Sight
LTE	Long Term Evolution
MAC	Medium Access Control
MCS	Modulation Coding Scheme
ME	Mobile Equipment
MIMO	Multiple Input Multiple Output
MISO	Multiple Input Single Output
ML	Maximum-Likelihood
MMSE	Minimum Mean Square Error
MPC	Multi-Path Component
MRC	Maximum Ration Combining
MSE	Mean Square Error
NLOS	Non-Line-of-Sight
OFDM	Orthogonal Frequency Division Multiplexing
OFDMA	Orthogonal Frequency Division Multiple Access
PARC	Per-Antenna Rate Control
PAPR	Peak-to-Average Power Ratio
PCI	Precoding Information
PDCCH	Physical Downlink Control Channel
PDSCH	Physical Downlink Shared Channel
RF	Radio frequency
RNC	Radio Network Controller
RRC	Radio Resource Control

RSRP	Reference Signal Received Power
RX	Receiver
SD	Sphere Decoding
SM	Spatial Multiplexing
SC-FDMA	Single-Carrier FDMA
SIMO	Single Input Multiple Output
SISO	Single Input Single Output
SINR	Signal to Noise-plus-Interference Ratio
SNR	Signal to Noise Ratio
SC	Sphere Constraint
TCP	Transmission Control Protocol
TDD	Time Division Duplex
TTI	Transmission Time Interval
TX	Transmitter
UDP	User Datagram Protocol
UE	User Equipment
UMTS	Universal Mobile Telecommunications System
WCDMA	Wideband Code Division Multiple Access
XPD	Cross Polarization Discrimination
ZF	Zero-Forcing

1. INTRODUCTION

Mobile telecommunications service providers have seen rapidly increasing demand for mobile data over past few years. This trend seems to be ongoing and increasing due to growing demands of packet switched data usage with various mobile devices. Main reasons for this growth are changes in user behavior and demands, increase in size of Internet and multimedia contents and aggressive marketing of wireless broadband connections with flat pricing schemes and simple device installations. Network operators have been forced to invest and seek new solutions to increase capacity and transfer rates they can offer to their subscribers [1]. One scheme used to provide more capacity is Multiple Input Multiple Output (MIMO), which utilizes multiple transmit and receive antennas to increase performance of wireless transmission in terms of capacity and peak rates.

MIMO has been introduced in latest evolution of Third Generation (3G) and Long Term Evolution (LTE) mobile technologies to improve capacity, spectral efficiency and data transfer rates operators can provide in cellular networks. As a technology, MIMO is specially suitable for wireless communications, because it can offer significant increases in both data throughput and link range without additional bandwidth or transmit power. Best performance gains from MIMO are experienced with high Signal to Interference-plus-Noise ratio (SINR) cases [2].

Most of the packet based data traffic generated in urban environment is originating from indoor environments. As demands for capacity are getting higher, network operators need to invest on efficient solutions to provide better coverage and capacity for indoor users, since outdoor macrocells and microcells providing indoor coverage often suffer poor results to end user performance. This can be solved by using dedicated indoor network solutions, such as indoor distributed antenna systems (DAS), and using latest evolution of mobile technologies. Proper indoor planning and antenna placements are crucial for obtaining best benefits from MIMO setup [3].

Rich scattering environments like indoor areas, are especially suitable for MIMO systems due to assurance of multipath propagation. Particularly attractive cases are narrowband propagation environments, where multipath creates independent channels even with small separations of antenna spacing. This makes orthogonal frequency division multiplexing (OFDM) modulation used in LTE a good match with indoor MIMO system [4].

This Master of Science thesis focuses on indoor performance of MIMO setup, introduced by the 3rd Generation Partnership Project (3GPP) releases for Evolved High-Speed Packet Access (HSPA+) and Long Term Evolution (LTE). Goal is to review indoor MIMO concepts, perform indoor field measurements and result analysis of MIMO performance

in different cases. Chapter 2 introduces basic principles of Multi-antenna concept and Chapter 3 focuses on indoor environment and its effect on MIMO channels and signal propagation. Closer look for HSPA+ and LTE performance and MIMO scheme is provided in Chapters 4 & 5. The measurement plan, equipment and software are introduced in Chapter 6. Chapter 7 provides the presentation of measurement results, comparison between test cases and analytical observations gathered from results and measurements. Finally Chapter 8 provides conclusions and summary based on studies and measurements, providing a good overview of key points of the topics and gathered results.

2. MULTI-ANTENNA TECHNIQUES

The idea of using multiple receive and transmit antennas has emerged as one of the most significant technical breakthroughs in modern wireless communications. Background principles of multi-antenna techniques originates from early 1990's. First US patent was proposed in 1993, considering concept of spatial multiplexing (SM) using MIMO and specially emphasizing applications to wireless broadcast methods [5]. First research work to refine new approaches to MIMO technology was done in 1996 and first laboratory prototype of spatial multiplexing was demonstrated in Bell Labs in 1998.

These first steps of MIMO research focused on improving link throughput and exploring other benefits and possibilities that MIMO based transmissions can provide in wireless environment [6, 7, 8]. First uses of MIMO utilized simple spatial multiplexing and experienced some gains from spatial diversity. More efficient use of multi-antenna techniques require more complex designs including advanced detection methods and more processing capabilities. Basic MIMO concept where each signal component experiences unique channel propagation conditions is illustrated in figure 2.1.

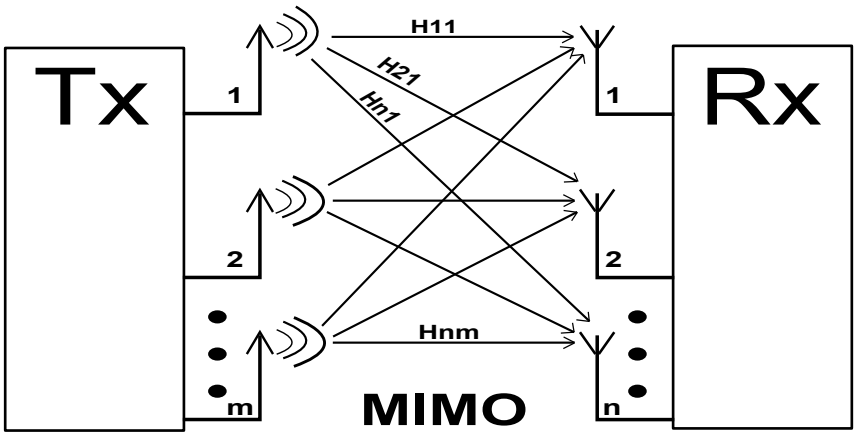

Figure 2.1: *Basic MIMO concept where each signal experiences different channel.*

Wireless transmission channel is affected by fading that impacts the signal to noise ratio (SNR). When SNR drops, error rate will increase in case of digital data transfer. The principle of diversity is to provide the receiver with multiple versions of same signal experiencing different channel conditions. With multiple diverse signals, the probability of similar channel conditions effects is reduced. This helps to stabilize the wireless link, improves performance and reduces error rates. In MIMO setup each antenna is a separate single element and have to be considered independently. It should not be treated as an

antenna array, where all antenna elements act as a single stream. The additional diversity against radio channel fading are provided with spatial diversity, where there is sufficiently large distance between antenna elements, and by polarization diversity, where antennas use different antenna polarization directions.

2.1 MIMO formats

There are different MIMO configurations that can be used. These different formats offer different advantages and disadvantages. The optimum solution is depending on the application. Terminology of these different form of antenna technology refer to single or multiple inputs and outputs. Basic concept of each implementation is shown in figure 2.2.

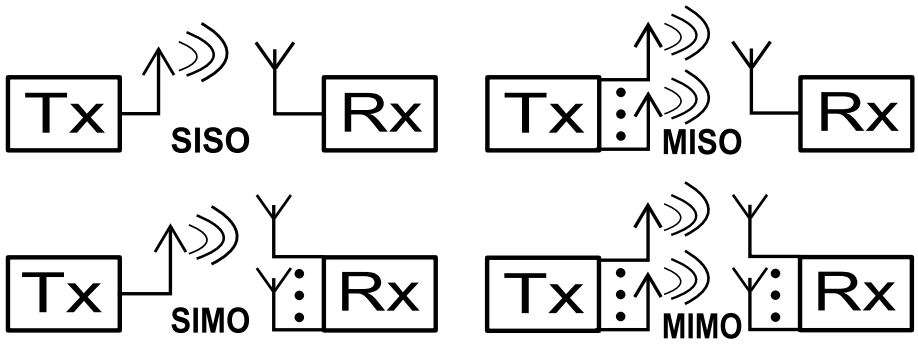

Figure 2.2: *Illustration of different antenna setups.*

Different MIMO formats all have different uses. The decision between different configurations needs to account the cost of additional processing and number of antenna elements needed versus performance improvements more complex systems can provide. Also in case of mobile equipments (MEs), the battery life limitations need to be weighted in the decision making. More antenna elements and heavier processing are directly increasing the power consumption of the mobile devices.

2.1.1 Single Input Single Output

Single Input Single Output (SISO) can be considered the most simple form of radio link. This case is effectively a standard radio channel. One transmitter antenna operates with one receiver. There is no diversity gains and no additional processing required. Advantage of SISO system is the simplicity. However, the SISO channel is limited on its performance. It is more susceptible to fading and interference than system using some form of diversity. Also the channel bandwidth of SISO is limited by Shannon's law [9].

2.1.2 Single Input Multiple Output

Single Input Multiple Output (SIMO) version of the MIMO is a case where transmitter has a single antenna and the receiver has multiple antennas. This case is also known as receive

diversity. SIMO is used to enable receiver to receive signals from multiple independent sources to gain diversity against fading effects. Advantage of SIMO is that it is relatively easy to implement. It requires no changes from transmitter, but some extra processing is required in the receiver end. The use of SIMO is suitable for many applications. Main limitations for it are cases when receiver is mobile device, where levels of processing are limited by size, cost and battery drain, and spatial difference between antenna elements is small. There are two main detection methods for SIMO. Switched diversity form is where SIMO system looks for the strongest signal between antennas and switches to that antenna. Maximum ratio combining (MRC) form takes all received signals from multiple receive antennas and sums them to a combination. In this form, all the received signals contribute to overall signal and improve SNR [9].

2.1.3 Multiple Input Single Output

Multiple Input Single Output (MISO) is another version of MIMO offering transmit diversity. MISO scheme is similar to SIMO, but in case of MISO the same data is transmitted from multiple antennas. The transmission redundancy allows receiver to be able to detect combination of transmitted signals, allowing increased total signal power and more diverse propagation and polarization. The advantage of using MISO is that multiple antennas are located at transmitter end, and the diversity processing is performed there. This allows reducing the receiver complexity, making MISO scheme suitable for transmitting data to mobile devices that have limitations in size or processing capabilities. Gain seen in MISO case is better SNR when best signal is chosen at receiver end [9].

2.1.4 Multiple Input Multiple Ouput

Multiple Input Multiple Output (MIMO) term is used when there are more than one antenna at both end of the radio link. MIMO can be used to provide gains in both channel robustness and channel throughput. Unlike degenerate cases of MIMO introduced previously, a large data throughput capacity increase is possible in case of MIMO. This requires dividing transmitted data to different groups and to use coding for separating the different channel paths. In case of MIMO, the complexity is greatest, because multiple antenna elements are required in both ends of the channel, and it requires heaviest amount of signal processing. But MIMO setup has capability to provide best gains in performance and capacity.

2.2 Capacity of wireless channels

Famous Shannon's Theorem in [10], provides a simple formula to calculate theoretical upper bound to the capacity of a link. The formula acts as a function of available bandwidth and SNR of the link. Result is given in bits per second. Shannon's Theorem can be stated

as:

$$C = B \cdot log_2 \left(1 + \frac{S}{N}\right), \tag{2.1}$$

where C is highest theoretical channel capacity, B is bandwidth of the channel in hertz, S is average signal power given in watts or in volt^{2}s and N is the average noise power, also in watts or volt^{2}s. From equation 2.1, it is clear that two fundamental factors limiting the capacity are the SNR and available bandwidth. The received signal power can be expressed as $S = E_b \cdot R$, where E_b is the received energy per information bit, and R is used bit rate. Furthermore, the noise power can be expressed as $N = N_0 \cdot B$, where N_0 is constant noise power spectral density reported in W/Hz [11]. This way the equation 2.1 can be expressed as:

$$C = B \cdot log_2 \left(1 + \frac{E_b \cdot R}{N_0 \cdot B}\right). \tag{2.2}$$

Additionally, by defining term bandwidth utilization $\gamma = R/B$. Because information rate can never exceed the maximum channel capacity, we get $R \leq C$. Now the bandwidth utilization formula based on Shannon's Theorem can be expressed as:

$$\gamma \leq log_2 \left(1 + \gamma \cdot \frac{E_b}{N_0}\right). \tag{2.3}$$

The channel utilization parameter and derived equation are useful for comparing capacity benefits gained from different MIMO setups. One way to increase the channel capacity is by using a high order modulation schemes, which are more sensitive to SNR than lower order modulations. Increase in transmit power is another method to boost channel capacity, because it increases the received signal power compared to noise power. However, the non-ideality of power amplifiers are limiting the range of practical signal power. Also in practical cellular networks, the interference is limiting the capacity, causing limitations of usable transmission power levels. Obtaining certain capacity is always a balance between allowable error rate, bandwidth, SNR and available transmit power.

2.2.1 Capacity increase through the use of MIMO systems

In MIMO systems, the principle is to establish multiple parallel subchannels, which operate simultaneously in same frequency and time domain. Since the correlation of subchannels is always between 0 and 1, it is possible to derive upper and lower bound of capacity. When signal propagation loss is not taken in to account, the maximum capacity is achieved when correlation between subchannels is 0. The worst case is when correlation factor is 1, meaning that all subchannels are interfering each other [12]. The maximum capacity for MIMO can be derived from equation 2.3 as:

$$\gamma_{max} \leq n_{min} \cdot log_2 \left(1 + \frac{\rho}{n_T}\right), \tag{2.4}$$

where n_T is number of transmitting antennas, n_R number of receiving antennas and $n_{min} = min(n_T, n_R)$. Additionally ρ is defined as:

$$\rho = \frac{P_{Tx}}{N^2} \cdot b, \tag{2.5}$$

where P_{Tx} is total transmit power, $N$is total noise power and *b* is defined as:

$$b^2 = \frac{1}{n_T n_R} \cdot \sum_{m=1}^{n_R} \sum_{n=1}^{n_T} |T_{mn}|^2, \tag{2.6}$$

where T is a matrix containing the channel transfer gains for each antenna pair. The minimal MIMO capacity is correspondingly:

$$\gamma_{min} \leq log_2 \left(1 + n_{min} \cdot \frac{\rho}{n_T}\right). \tag{2.7}$$

From these formulas 2.4 and 2.7,it can be clearly seen that the benefits from MIMO in capacity increase is strongly connected to the correlation between subchannels.

2.2.2 Waterfilling

When the transmitter has knowledge between the correlations of subchannels, the power can be allocated in optimal way using the distribution known as waterfilling. The waterfilling distribution scheme allows system to obtain maximum possible capacity based on specific system conditions. The basic concept of waterfilling is to divide the transmit power for all different subchannels in a way, that each channel reaches the required level of SNR. Basically this means that channels with more attenuations get more transmit power to compensate SNR levels at receiver end. If a channel condition is really poor, the waterfilling algorithm discards the use of that subchannel until its condition improves [13].

One of the most common difficulty with waterfilling algorithm in case of MIMO is used method of the minimization of the sum of mean square errors (MSEs) of different subchannels within MIMO channel. Instead of performing minimizing the sum of MSEs, system should be designed to minimize the determinant of the MSE matrix. This allows classical capacity-achieving waterfilling result to be obtained in MIMO systems. The most common methods to utilize waterfilling solutions are balancing SINR ratio between subchannels, minimizing MSE matrix determinant or minimizing average bit error rate (BER) over a set of parallel subchannels. The minimization of average BER is most suited, when there is least channel knowledge [14].

2.3 Spatial multiplexing

Spatial multiplexing is a transmission technique utilized in wireless MIMO communication. The term spatial multiplexing means reusing of space dimension, by transmit-

ting independent and separately encoded data signals, called streams, from each of the multiple transmit antennas. The maximum SM order, describing number of streams, is $N_s = min(N_t, N_r)$. Figure 2.3 illustrates basic idea of MIMO using SM.

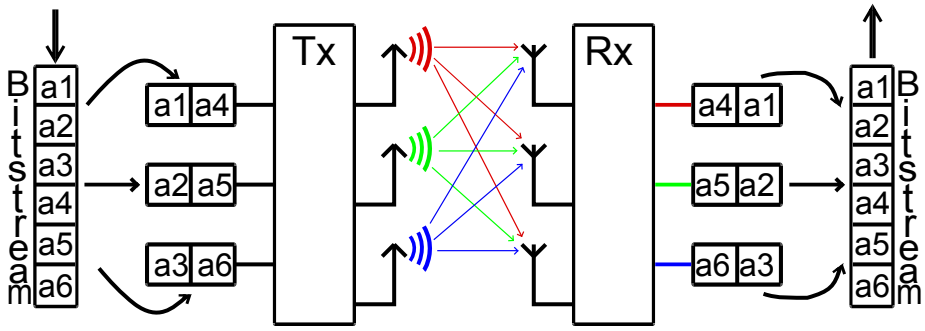

Figure 2.3: *Third order Spatial Multiplexing example.*

The theoretical gain of SM is the basic SISO case throughput $R_{SISO} \cdot N_s$, because in ideal case the bitstream rate, or correspondingly spectral efficiency, can be increased by the factor of SM order.

The basic principles how multiple parallel channels can be created in case of MIMO using for example in 2×2 antenna configuration is presented in equation 2.8. The received signals can be expressed as:

$$\overline{r} = \begin{bmatrix} r1 \\ r2 \end{bmatrix} = \begin{bmatrix} h11 & h12 \\ h21 & h22 \end{bmatrix} \cdot \begin{bmatrix} s1 \\ s2 \end{bmatrix} + \begin{bmatrix} n1 \\ n2 \end{bmatrix} = H \cdot \overline{s} + \overline{n}, \tag{2.8}$$

where $\overline{r}$ is received signal vector, H is the channel matrix, $\overline{s}$ is transmitted signal vector and $\overline{n}$ is noise vector. Assuming noise vector is 0, and that the channel matrix H is invertible, the signal vector $\overline{s}$ can be recovered perfectly at the receiver by multiplying the received vector $\overline{r}$ by with matrix $W = H^{-1}$ [11].

In case of excess antennas in transmitter, they can be used to provide beam-forming to provide additional gain for reception. Combining SM and beam-forming can be achieved by means of *pre-coder-based* SM. Linear precoding can be done by means of a size $N_T \times N_L$ precoding matrix in transmitter, where N_L is number of signals to transmit and N_T is number of transmit antennas. In practical cases N_L is equal or smaller than N_T, meaning that N_L signals are transmitted by using N_T transmit antennas [11].

When $N_L = N_T$, the precoding matrix is used to provide orthogonality to parallel transmissions, increasing signal isolation and thus reducing inter symbol interference (ISI) at the receiver end. When the number of signals to be transmitted is less than number of transmit antennas $(N_L < N_T)$, the precoding in addition provides possibility for beam-forming in combination of spatial multiplexing. In practice, the precoding matrix will never perfectly match the channel, thus there will always be some residual interference between transmitted signals. However, this interference can be taken care of by additional processing at receiver end [11].

The channel matrix H can be expressed in precoding case as:

$$H = W \cdot \sum \cdot V^H, \tag{2.9}$$

where columns V and W are coding matrices,$\sum$ is a $N_L \times N_L$ diagonal matrix with the N_L strongest eigenvalues of H^H as its diagonal elements [11]. Figure 2.4 demonstrates the use of precoding elements in transmission.

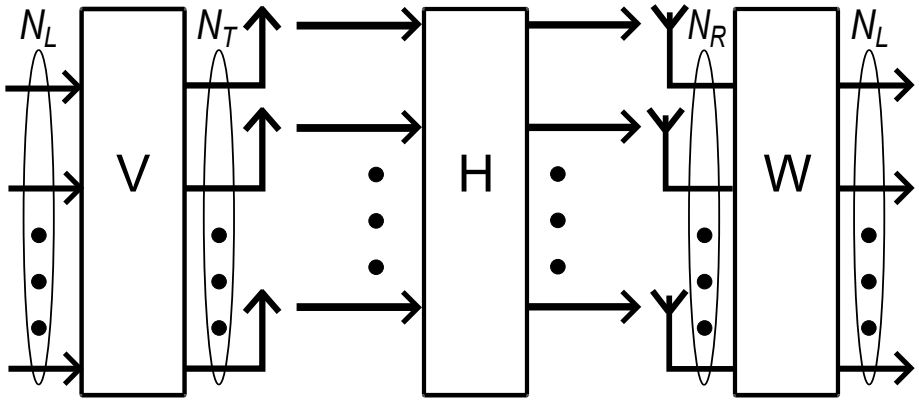

Figure 2.4: *Orthogonalization of spatially multiplexed signals by means of precoding.*

To determine suitable precoding matrices V and W, the knowledge of channel H is needed. A common approach is to have receiver estimate the channel and decide suitable matrix from a set of available precoding matrices. Then the receiver gives feedback information about the selected coding matrix to transmitter for it to choose suitable matrix V based on channel conditions [11].

2.4 Spatial and polarization diversity

Spatial diversity method for SM requires distance between transmitting antennas. Typically required distance between antenna elements would be in magnitude of wavelength (λ) of transmitted signal. Bigger distance between antennas helps to ensure more uncorrelated radio channel propagation for separate parallel signals from different transmission antennas. In case of spatial diversity transmission, the antennas have usually same polarization.

Polarization diversity refers to the transmission scheme where signals are transmitted and received simultaneously on orthogonally polarized waves. Polarization of electromagnetic wave is defined as direction of its electric field vector. Diversity gain can also be achieved from polarized parallel channels without any requirement of spatial separation. Polarization diversity is an attractive alternative compared to spatial diversity. It does not require transmitting antenna elements to be separated by distance, thus the polarization can be performed with polarized antennas in single antenna element. In practice, two polarization schemes are most commonly used: horizontal / vertical (0° / 90°) or slanted

(+45° / -45°) [15].

Polarization scheme, however, is only suitable for 2 × 2 MIMO, because 90° angle difference in transmission polarization is required to achieve orthogonal Independence between transmitting antennas. For higher order SM, there can also be hybrid cases of spatial and polarization difference. In case of 4 × 4 MIMO, the diversity could be obtained with two antenna elements with spatial distance and both using polarized antenna implementations [15]. Figure 2.5 shows simplified case of hybrid diversity method. In the figure

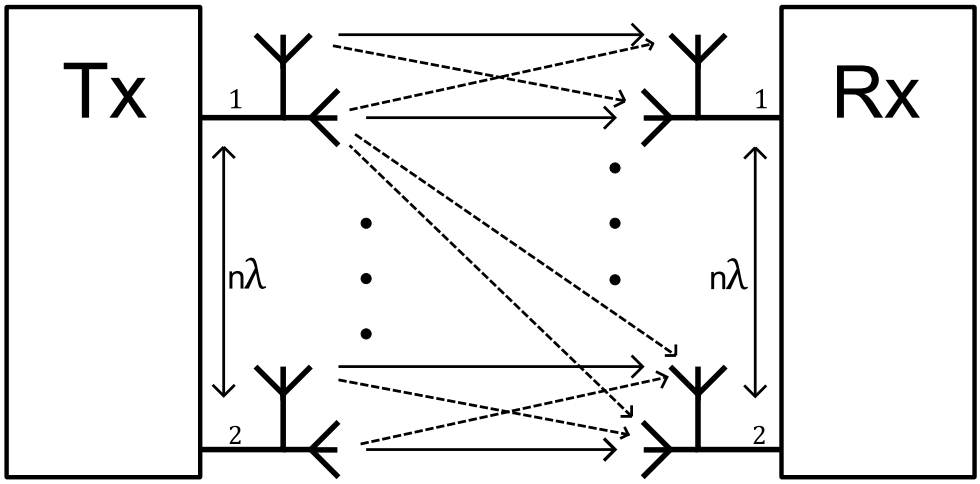

Figure 2.5: *Example of 4 × 4 MIMO with hybrid spatial and polarization diversity.*

all channels are separated either with spatial diversity or polarization diversity. Hybrid design helps to reduce amount of antenna elements, while still offering higher order SM capabilities.

In case of spatial diversity, the main affecting factor is the distance between antennas. Distance separation can be done in transmitting, receiving or both ends. In practical cases with fixed base transceiver station (BTS) locations and mobile UEs, the transmitter spacial distance is only possible to obtain in BTS end. Small sized mobile stations can not fit antenna distances of several wavelengths. The polarization diversity offers solution for space problems. However, the affecting factor for polarization diversity performance is cross polarization discrimination (XPD) [15].

XPD measures the extent of depolarization in a wireless channel. It is defined as:

$$XPD = 20 \cdot log\left(\frac{Ec}{Ex}\right) \quad dB, \tag{2.10}$$

where Ec is co-polar signal strength and Ex is the cross-polar signal strength at receiver. High values of XPD indicate higher lever of separation between different polarizations. Higher separation implies better suitability for polarization diversity in multiplexing techniques. However, specially in NLOS scenarios, high XPD ratio causes diversity deficit for polarization diversity based MIMO systems. It is shown in [16], that MIMO system capacity is reduced for high level of XPD, because it means less signal scatters and reflections

over wireless channel, causing less multi-path components (MPC). Different wireless environments have different impacts of XPD behavior over propagation channel. Based on [17], the best polarization diversity gains are obtained in small cells that offer many scattered signals. This ensures multiple received signals with similar signal strengths, delay and random polarization.

2.5 Reception schemes

There are different reception schemes in order to detect and receive correct wanted signal at receiver. Choosing the reception method depends on implementation and complexity of the receiver and transmission conditions in wireless environment. The optimal solutions are usually most complex to implement and can require more processing than simpler solutions. Linear schemes are usually based on zero-forcing (ZF) or minimum mean square error (MMSE) criterion. Non-linear receiver processing are using various implementations like maximum-likelihood (ML) or successive interference cancellation (SIC) [18].

Obtaining knowledge of the channel is important for reception. In 3G and LTE systems, the channel estimation in receiver is based on pilot or reference signal analysis. When known pilot symbol is sent through the channel, the distortion effect can be seen and channel equalizer configured to negate the effect of phase and amplitude changes.

2.5.1 Zero-Forcing and Minimum Mean Square Error

Linear receivers like ZF or MMSE provide sub-optimal performance, but offer significant reduction to computational complexity with tolerable performance degradation. In these schemes, the accurate knowledge of channel is essential for proper operation. In practice, the accurate knowledge of channel is not always available to transmitter, which can have negative effect on performance of linear MIMO receivers, if the optimal precoding matrix is not used [19].

The ZF and MMSE equalizers can be applied to decouple N substreams. The equation for ZF and MMSE matrices are:

$$W_{zf} = (H^*H)^{-1}H^*, \ \ and \quad W_{mmse} = \left(H^*H + \frac{1}{snr}I\right), \tag{2.11}$$

where W_{zf} or W_{mmse} are used in receiver to multiply the received signal vector to cancel the channel H effects. Term I in equation 2.11 is identity matrix, with ones in diagonal and zeros elsewhere. The marking H^* denotes the complex conjugate of matrix H. More accurate the channel H knowledge is on W matrices, better the detection accuracy is [20].

2.5.2 Maximum-Likelihood detection

ML detection is considered optimal receiver approach for spatially multiplexed signals. The performance of other reception scheme is usually compared against ML. The limi-

tations of ML is, that in many cases it is too complex to implement in practical systems. The optimal detection of signals transmitted over MIMO channels is known to be a NP-complete problem, meaning it cannot be solved by computating methods using reasonable amount of time [21].

Basic concept of linear MIMO communication system is where transmitted symbol vector $\overline{s}$ is multiplied by channel matrix H, and noise n is added to the signal. This gives us a received symbol vector $\overline{v}$ that arrives at detector. After detection, the symbol vector $\hat{s}$ is chosen for output. The detectors role is to choose one of the possible transmitted symbol vectors based on available data. The optimal detector should return $\hat{s} = s_*$, the symbol vector whose probability of having been sent, given the observed vector $\overline{v}$, is the largest. This is known as the Maximum A posteriori Probability (MAP) detection rule. Equation is give as:

$$s_* = argmax P\left(\overline{s}\ \ was\ \ sent \,|\, \overline{v}\ \ is\ \ observed\right), \tag{2.12}$$

where $\overline{s}$ is part of known and finite symbol alphabet. In practical case, assumption is that $P(\overline{s}\ \ was\ \ sent)$ is constant, then the optimal MAP detection rule can be written as:

$$s_* = argmax P\left(\overline{v}\ \ is\ \ observed \,|\, \overline{s}\ \ was\ \ sent\right). \tag{2.13}$$

A detector that always returns an optimal solution satisfying equation 2.13, is called ML detector [21].

2.5.3 Successive Interference Cancellation

Successive interference cancellation is non-linear approach for demodulation of spatially multiplexed signals. It is based on an assumption that the signals are separately coded before the spatial multiplexing, often referred as *Multi-Codeword* transmission. The figure 2.6 illustrates the basic concept of SIC scheme, where received signals are demodulated in successive order.
In the SIC detection, the first signal is demodulated, decoded and re-encoded, then its subtracted from received signals. In ideal case all the interference from first signal is removed from rest of the signals. This interference reduction continues in successive order until all signals have been demodulated and decoded [11].

For the first signals decoded in case of SIC, it is clear that they are subject to higher interference levels, compared to later decoded signals. This phenomenon requires differentiation in the robustness of different signals, so that first signals in decoding should be more robust to interference than second one, and so on. This can be achieved for example by applying different modulations and coding rates to different signals. Lower-order modulations and lower coding rates to combat interference. This method is referred to as Per-Antenna Rate Control (PARC) [22].

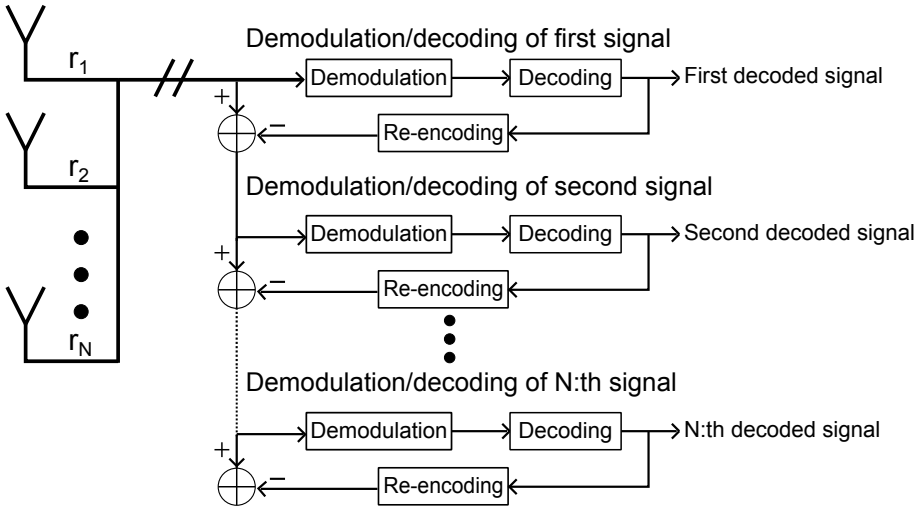

Figure 2.6: *Demodulation of spatially multiplexed signals based on Successive Interference Cancellation.*

2.5.4 Sphere Decoder

The main idea in Sphere decoding (SD) is to reduce the number of candidate vector symbols to be considered in the search that solves ML solution. This is achieved by constraining the search to only those points that are inside a hypersphere with radius r around the received point y. The corresponding idea is referred to as the sphere constraint (SC):

$$d(s) < r^2 \ \ with \ \ d(s) = ||y - Hs||^2, \tag{2.14}$$

where $||y - Hs||^2$ is an alternate way to express the MAP detection shown in equation 2.13 [23].

Normally the SD is implemented as a depth first tree search, where each level in the search represents on transmitted signal. Figure 2.7 illustrates this scheme, where branches exceeding the radius constraints can be discarded from consideration. The estimation of how much the trees need to be searched in advance is difficult, since it is affected by noise and channel conditions. This is why the complexity of sphere decoder is typically not fixed, but it varies with time.

The issue with SD is that with many antennas and high order modulations the computation requirements grow exponentially. There are proposals for dealing with this issue, such as using parallel processing to speed up the throughput of sphere decoders. This implementation is used to 'split' the sphere trees into subtrees and compute the route in parallel with multiple subtrees. Faster performance, and thus higher throughput can be achieved, but this requires more computation effort with parallel calculations [24].

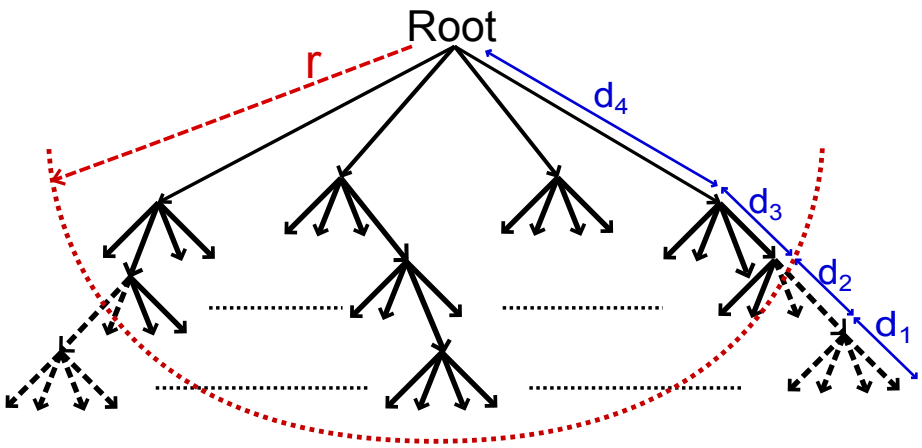

Figure 2.7: *The structure and Sphere Constraint for Sphere Decoder.*

2.5.5 Alamouti code

One widely used MIMO detection method is space-time code. With space-time codes, one data stream is transmitted from multiple antennas, and the signal is coded to exploit independent fading conditions multiple antennas can achieve with spatial diversity. Most popular space-time code is Alamouti, which is used in many wireless standards [25]. Typical Alamouti code in case of 2×2 MIMO can be expressed as:

$$\begin{bmatrix} y_{0,0} & y_{0,1} \\ y_{1,0} & y_{1,1} \end{bmatrix} = \begin{bmatrix} h_{0,0} & h_{0,1} \\ h_{1,0} & h_{1,1} \end{bmatrix} \begin{bmatrix} x_0 & -x_1^* \\ x_1 & x_0^* \end{bmatrix} + \begin{bmatrix} n_{0,0} & n_{0,1} \\ n_{1,0} & n_{1,1} \end{bmatrix}, \tag{2.15}$$

and rearranged from equation 2.15 to:

$$\begin{bmatrix} y_{0,0} \\ y_{1,0} \\ y_{0,1}^* \\ y_{1,1}^* \end{bmatrix} = \begin{bmatrix} h_{0,0} & h_{0,1} \\ h_{1,0} & h_{1,1} \\ h_{0,1} & -h_{0,0}^* \\ h_{1,1} & -h_{1,0}^* \end{bmatrix} \begin{bmatrix} x_0 \\ x_1 \end{bmatrix} + \begin{bmatrix} n_{0,0} \\ n_{1,0} \\ n_{0,1}^* \\ n_{1,1}^* \end{bmatrix}. \tag{2.16}$$

The equation 2.16 implies that signals x_0 and x_1 are transmitted in two orthogonal paths. Therefore, they can be detected independently, and only simple linear processing is required.

The benefits of Alamouti code is that it provides higher diversity gain and does not require complicated detection. Disadvantage compared to SM case is that Alamouti code transmits only single data stream instead of multiple streams. This makes Alamouti code more suitable in worse channel conditions, where SNR is too low to utilize multiple streams for capacity gain effectively. And for cases where channel is very singular and thus unsuitable for SM scheme. Many wireless standards have adopted both schemes to dynamically adjust wireless transmission method based on existing channel conditions [25].

2.6 Open-loop and closed-loop approach

There are two types of transmit spatial diversity, open-loop and closed-loop. The term *open-loop* is used when there is no feedback information about channel and interference conditions between transmitter and receiver. *Closed-loop* term implies that there is a constant feedback from receiver, that allows transmitter to adjust transmitted signals to cope better experienced channel conditions. Open-loop transmit involves transmitting signals from multiple antennas in deterministic pattern, that does not depend on channel. There are advantages and disadvantages for both cases. Most current wireless standards include support for limited feedback schemes. For example, channel state information (CSI) that can be used in High Speed Downlink Packet Access (HSDPA) and LTE for closed-loop transmission.

In order to avoid heavy overheads from closed-loop feedback for the system uplink, channel information is usually quantized. This method is called limited feedback. Another issue with closed-loop feedback solutions is the delay. It is not a problem in slow-fading channels, but in fast-moving environment the channel becomes fast fading, and the feedback delay can cause closed-loop MIMO significant performance losses. Another way to obtain CSI is by uplink sounding, when ME transmits a sounding signal to BTS. Then the BTS can utilize the received signal to obtain information about channel, without extra delays, and does not require a dedicated feedback channel. However this method is mostly suitable for TDD systems, where uplink and downlink use same frequency bands. When used in FDD system, different frequencies typically experience different channel properties. This causes performance losses for uplink sounding in case of FDD [26, 27].

3. INDOOR ENVIRONMENT

Indoor as an environment for wireless transmissions compared to outdoor propagation environment offers different approaches for the planning process. In smaller cells like pico- or even femtocell, the coverage is usually not an issue. The focus is more on limiting the coverage to desired locations and preventing interference to neighboring cells. Because the distances between BTS antenna and mobile user equipment (UE) are short, the propagation loss is lower than in outdoor environments with longer distances. Also fast fading effects are less in indoor environment, where objects are mostly fixed and movement speed of UEs are slow.

Time variations within indoor systems are much less than outdoor mobile systems. Spreading in frequency domain, also known as Doppler spreading, in a typical wireless indoor system can be discarded. Indoor areas also typically experience more and stronger MPCs. All these things make indoor environment very suitable for MIMO schemes. Best benefits from MIMO can be achieved with high SNR values and with rich multipath environment, ensuring better detection capabilities and performance for SM and other multi-antenna techniques.

3.1 Signal propagation and channel model

There are numerous radio propagation models, that aim to predict radio wave propagation in wireless environments. Many of them are involved around "free space" radio wave propagation, also known as free-space path loss (FSPL), or free-space loss (FSL), where electromagnetic wave travels in straight line through free space with no obstacles. The FSPL equation is expressed as:

$$L_{fs} = 32.45 + 20 \cdot log(d_{km}) + 20 \cdot log(f_{MHz}), \tag{3.1}$$

where d_{km} is distance between antennas in kilometers and f_{MHz} is used frequency in MHz [28].

The ideal propagation is not usually experienced in practical cases, so models need to tune other parameters based on environments, frequencies and different correction factors for specific models. The basic phenomenons that affect radio propagation and cause signal distortions and losses are reflection, diffraction, scattering and penetration. Different objects and materials have different affects on radio signals. Additionally, the angle and polarization of the signal hitting an obstacle affects the strength and phase of the reflecting

or scattering signal.

The main difference between signal propagation in outdoor and indoor is that an outdoor environment is more easily predictable and there are topographical maps and databases that accurately determine the shape of an outdoor cell. Using mapping and database approach for modeling is not feasible in indoor systems. Indoor models are not accurate enough to predict and account every factor affecting signal propagation happening indoors. This makes indoor propagation modeling less accurate, because wireless channel behavior can be more unpredictable and experience strong changes within small distances.

3.1.1 Noise and interference

All signals in wireless radio channels are experiencing, in addition FSPL and propagation phenomenon, the effects of noise and interference. The interference is caused by man-made signals and phenomenon affecting in same frequency band as desired signal. Interference from other frequencies outside the used band can easily be dealt with bandpass filters. However, interfering signals in same frequency are disturbing the desired signal. One major difference between interference and noise is that interference typically has a certain structure and predictability, that can be exploited to suppress or remove its effect completely. For example, multiple access schemes such as WCDMA and OFDMA have different approaches how to deal with interfering signals through the use of coding and orthogonality between subcarriers [11].

Noise effect is affected from both human and natural sources. Electromagnetic background radiation is caused by sun and stars and other celestial objects. Thermal noise is affecting all electronic circuits that contain resistors. Effect of noise is usually modeled as *white noise*. It is defined by its frequency-domain characteristics. It has constant power in all frequencies, and at each frequency the phase of the noise spectrum is completely uncertain and is unrelated to phase at any other frequency. Amplifiers used in transmitters and receivers add to noise effect as they boost the amplitude of the signal experiencing additive noise. This is why filtering out unwanted bands is important to minimize noise effect in the wireless systems. Noise interference can not be removed or predicted in wireless communications. Wireless systems need to designed in such a way, that reliable communication can be achieved with channel experiencing noise effects. This can be ensured by having higher signal power compared to noise power at reception, or utilizing other methods, such as spreading and despreading in WCDMA.

3.1.2 Path loss

Deterministic approach such as ray tracing allows deterministic prediction of received signal level at certain location. Accurate prediction needs to account every object and their properties affecting the propagating signal from source to destination. When adding

the multipath propagation the amount of different paths radio waves can propagate, the complexity of accurate predictions increases radically. Indoor spaces containing lots of different types of objects and typically strong multipath propagation often makes purely deterministic path loss models, such as ray tracing or launching, impractical to be used [29].

An alternative to deterministic approach is to use an empirical (statistical) channel model for path loss estimation. Empirical models are based on parameters obtained from thorough measurement results with different environment types. For indoor environment, the empirical models take in to account various different parameters that can be tuned based on current setup. The general parameters are frequency range, bandwidth and type of environment. Also multipath propagation, short and long-term fluctuations have to be accounted. Indoor specific parameters are, for example, type of rooms, area or corridors, amount of objects affecting the propagation, type and thickness of materials used in walls and ceiling, and size and shape of building. Example of COST 231 model for indoor office propagation is given as:

$$L = L_{fs} + 37 + 3.4 \cdot K_{w1} + 6.9 \cdot K_{w2} + 18.3 \cdot n^{((n+2)/(n+1)-0.46)}, \tag{3.2}$$

where L is attenuation (path loss) in dB, $L_(fs)$ is FSL in dB, n is number of traversed floors, K_{w1} is number of light internal walls and K_{w2} is a number of thick internal walls [29].

3.1.3 Multipath propagation

Multipath propagation is result from several different obstacles and reflectors in radio channel. This makes received signal to arrive as a set of unpredictable reflections with different attenuation and delay behavior. Multipath waves in indoor environment tend to arrive in clusters. Within each cluster the delay differences are relatively small. Delays between the clusters are larger in comparison. The delay spread is a commonly used parameter to quantify multipath effects. Delay spread in indoor is usually small, rarely exceeding few hundred nanoseconds. Delay spread also increases with the distance from BTS [29]. Figure 3.1 shows example of delay spread effect in time and frequency domain.

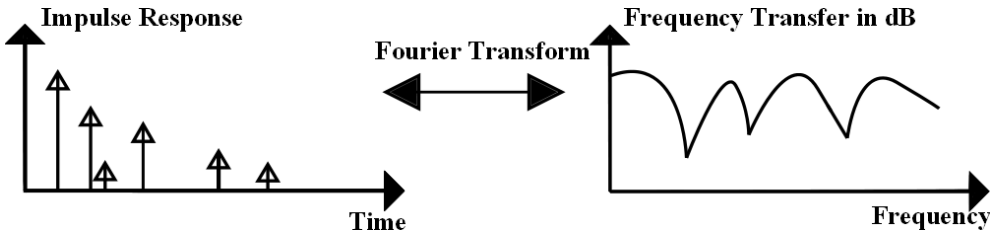

Figure 3.1: *Delay effect of multipath impulse response to frequency behavior.*

In multipath reception, Rayleigh fading model can be used to describe wireless radio channel, and allow calculations of outage probabilities and other link parameters. Rayleigh fading suggests, that mobile antenna receives continuously a large number of independent reflected and scattered waves with different phases and amplitudes. Because of wave cancellation and addition effects, the received power seen by a moving antenna at any given time becomes a random variable, depending on the location of mobile device. Rayleigh fading is usually used in NLOS cases, where there is no clearly dominant signal component.

Rician fading model is similar to that of Rayleigh model. In case of Rician fading, a strong dominant signal component is present. This dominant component is caused for example a LOS radio wave. The dominant wave component can be a sum of two or more dominant signals, for example LOS signal and nearby strong reflections. This combined dominant signal can be treated in a deterministic way. Both Rician and Rayleigh fading models can be used for indoor system, depending on the case of LOS or NLOS reception location.

The Rician K factor is defined as the ratio of dominant single power compared to other scattered and reflected signal components. It can be important value in estimation wireless channel behavior. The K factor determines the distribution of received signal amplitude, and can be useful in determining the BER or other useful metrics of a channel. Direct measurement of K factor is difficult, but it can be estimated, for example by using a set of different samples of the channel at different frequencies [29].

3.2 Indoor antennas

Correct antenna placement is very important in indoor areas. Possibilities for placement locations may be limited due various reasons, but difference between proper placement and poor placement can be significant for cell performance. Depending on type and size of indoor environment, the coverage can be provided with single omni-directional antenna, or multiple separate antennas, also known as DAS. In the studies for antenna location effects with MIMO performance [30], the results suggests that the capacity of indoor MIMO system is significantly affected by the antenna locations. Also notable conclusion is that if path loss is ignored, in NLOS case, the affect on MIMO channel capacity is almost independent of antenna locations. The highest capacity was obtained when transmitter antenna is located in center part of the wall. When antenna is moved towards edges and corners, the performance degrades.

Antenna placement in indoors also depends on the type of antenna. Directional antennas are often placed on outer walls directing the beam inside the building, while omni-directional antennas are more suitable to be placed in center area of building, and possibly on ceiling, to allow better LOS coverage. One other option to fixed point antennas is to use radiating cable antenna, often referred as radiating coaxial cable. This can be installed inside ceilings or walls and used to provide continuous coverage over longer distances.

The radiating cable antenna provides similar signal strength over whole length of its installation. The cell performance is thus depending on distance and obstacles between UE and any point of the radiating cable antenna.

The proper design and implementation for DAS system is important for indoor cell coverage and performance. When multiple antennas are used to provide sufficient coverage to whole building or just for specific locations inside the building, antenna locations should be distributed evenly around area. This allows to use less power for antennas and still provide good coverage and signal strengths over larger area. Figure 3.2 shows an example of simple DAS used in a building including cable losses and power distribution. The simplest way to implement DAS is to select antenna locations and then just install cables to each antenna using basic splitters that divide power equally for both outputs. It

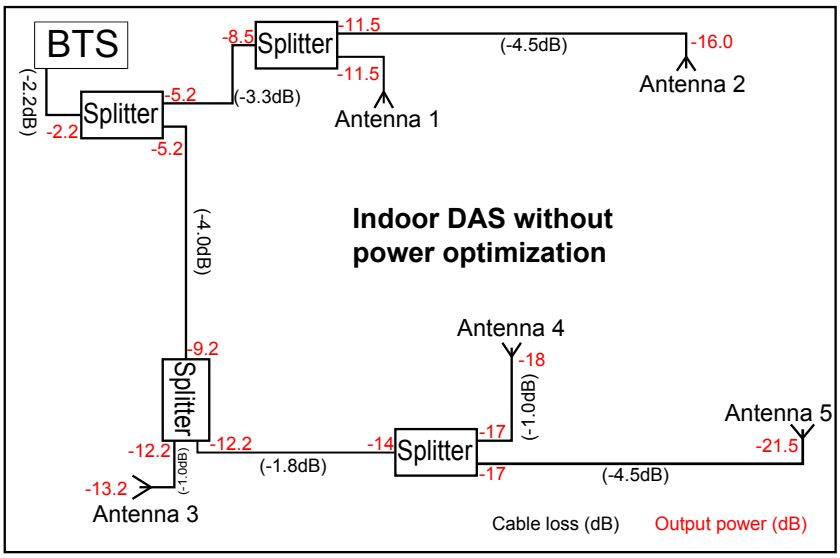

Figure 3.2: *Example of a simple indoor DAS setup.*

can be clearly seen that power levels between antennas close to BTS and further away are very different. This causes various issues between cells that have different coverages. From UE point of view, the dominant antenna can be further away than closest antenna to user location. This can cause increased interference levels for uplink, more handovers, poor performance and even dropped calls on weak coverage areas caused by bad power optimization in DAS setup [31].

The easiest way to balance the power levels between different antennas and fix the near/far problem is to use directional couplers. These act as splitters, but power levels are not divided equally. Different directional couplers have different ratios for the power division. By choosing most suitable components for cable installation, the power levels can be easily optimized to provide similar output power for all antennas in DAS setup. Figure 3.3 shows the optimization done with directional couplers for the case shown in figure 3.2. In the example case, the optimized DAS setup brought maximum antenna power difference from 10 dB to 1.1 dB, by replacing the splitters by directional couplers.

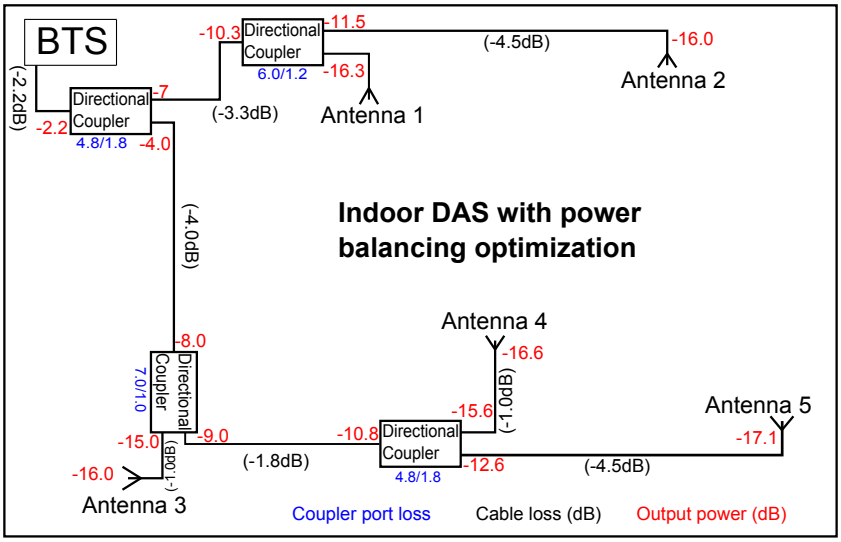

Figure 3.3: *Example of an optimized indoor DAS setup.*

As size of DAS grows, the number of antennas, lengths of cables and amount other radio frequency (RF) equipments, such as splitters or couplers, increases. This makes power balancing and optimization become more and more important for bigger setups. Each antenna should have sufficient power level to provide good enough SINR and balanced coverage areas [31].

4. HSPA+

High-Speed Packet Access (HSPA) and its evolution HSPA+ are 3GPP standards aimed to extend and improve existing wideband code division multiple access (WCDMA) protocols for Universal Mobile Telecommunications System (UMTS). The specification standard for HSPA+ was introduced in 3GPP Release 7 in 2007 and its worldwide commercial deployment began in 2010 and is still ongoing [1].

Later 3GPP releases define new features and offer advanced functionality for HSPA+. Recent 3GPP releases supporting HSPA / HSPA+ are often denoted as 3.5G and 3.75G, implying that they offer advanced features and performance for 3G, but are not considered as the 4th generation.

4.1 High speed packet access improvements for WCDMA

Latest releases for 3GPP WCDMA specification are generally referred as HSPA+. It is designed to bring further enchantments for packet-data services in WCDMA end-user performance and system level. First HSPA enchantments, in Release 5 & 6, introduced new basic methods, such as higher order modulation supporting 16-QAM, fast scheduling and rate control, possibility for faster 2 ms transmission time interval (TTI), and fast hybrid ARQ to improve capacity and reduce latency times compared to Release 99. The Release 7 introduced new HSPA+ features in WCDMA. The main features are option for MIMO usage, support for 64-QAM modulation and continuous packet connectivity scheme [11].

Releases 8 & 9 provide additional enchantments and features for HSPA+. 64-QAM modulation support for MIMO scheme is added in Release 8, in order to boost the peak downlink rates. A new technique called dual-carrier operation in downlink is also introduced in Release 8. It provides an option for two adjacent carrier frequencies to be used simultaneously, allowing 10 MHz bandwidth usage instead of 5 MHz. This technique can double the peak data rates and provide substantial increase in cell capacity [32].

However, the Dual-carrier scheme does not offer improvement in spectral efficiency like SM MIMO does, and some mobile operators do not have 10 MHz bandwidth license required for dual-carrier scheme. Release 9 allows different cells in multicarrier operation to exist in separate frequency bands and be used in combination with MIMO in downlink. Multicarrier operation in uplink is also introduced in Release 9, allowing to achieve higher peak rates while maintaining UE complexity level reasonable [32].

In addition to new features and schemes, also receiver equipment have experienced improvements. Mobile terminal needs GRAKE2+ (type3i) receiver for more advanced

features. Also transmission channels and states have experienced enchantments. The enchanted states aim to keep user in a state that offers best trade-off between data rate availability, latency and reaction times, and battery consumption. Common states with active Radio Resource Control (RRC) access are URA_PCH, CELL_PCH, CELL_FACH and CELL_DCH. Transitions trigger between states based on user requirements are made more efficient in HSPA+ [32, 11]. However, the exact timings and triggers for state transitions are vendor equipment and network operator specific.

4.2 MIMO with HSPA+

HSDPA-MIMO supports transmission of two streams simultaneously. Both streams are subject to same physical-layer processing in terms of coding, spreading and modulation as single-stream HSDPA case. For MIMO transmission, linear precoding is used before transmission. Precoding is beneficial even if only one stream is used, because it can provide diversity gain. The idea behind precoding is to pre-distort the signals that the two streams are as orthogonal as possible at the receiver end. The orthogonality reduces interference between two streams and eases processing requirements at receiver end [11].

The changes in physical-layer processing affected by the introduction of MIMO are relatively simple. And impact to the protocol layer is small. Figure 4.1 illustrates MIMO transmitter scheme used in HSPA+. All units in transmitter chain must be able to perform

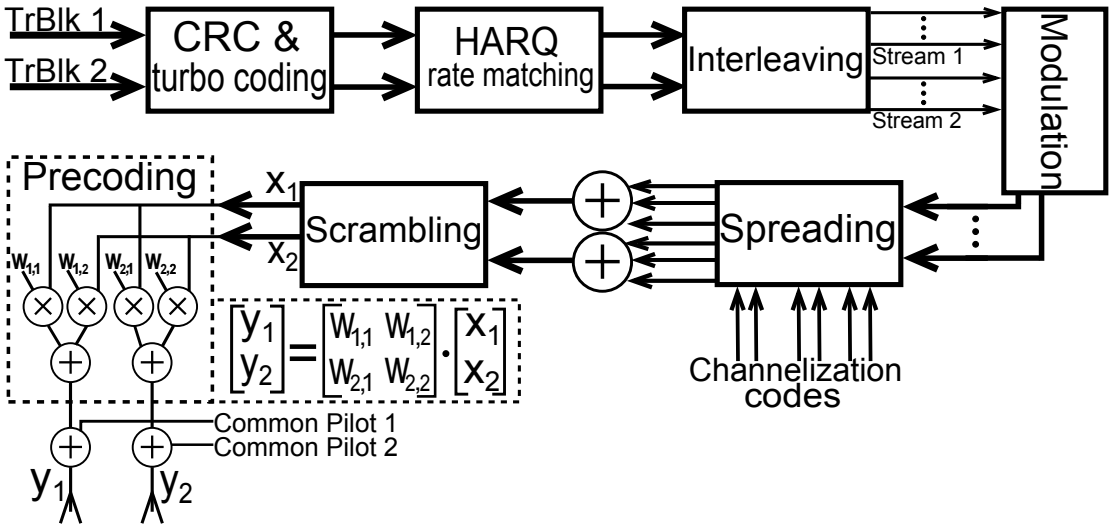

Figure 4.1: *MIMO transmitter chain for HSPA+*

the operations simultaneously for two separate transmission blocks. Transmitter chain consists of coding unit, that adds redundancy and error detection for bitstream. Hybrid automated repeat request (HARQ) is matched for each transmission block to add error correction bits for transmissions. In retransmissions, HARQ can generate different redundancy versions of same data, in order to obtain incremental redundancy for retransmissions. HARQ rate matching operates in two stages. First it is used to match the data

rate of incoming stream to the capacity of used Virtual Incremental Redundancy buffer, and then match the buffer capacity to physical channels. Interleaving is used to distribute symbols around the matrix in order to diminish the effect of fading or other interference that can cause bursty errors in transmission. With interleaving operation, the distribution of corrupted data symbols becomes more even, allowing error-correction schemes better change to recover original data [11, 33].

Modulator maps the data bit streams into symbol constellations. Modulation order is determined by channel quality. For worse channel conditions, smaller modulation is used to cope with the cases of stronger interference or path-loss. The modulated symbols are then spread by spreading factor 16. Number of spreading codes used is depending of how much capacity cell has to offer for HSDPA user, and is also based on user equipment capabilities. The amount of spreading codes for HSDPA use is between 1 and 15. More spreading codes allow more capacity for user data in one transmission block. After spreading, the data streams are scrambled in order to prevent interference from other cells. Each nearby cell has own unique scrambling code. This allows UE to separate simultaneous transmissions from neighboring cells [11].

The precoding operation for MIMO streams is straightforward. Both data blocks are multiplied by precoding matrix. The weights in precoding matrix are chosen in such way, that orthogonality is maximized between two streams in receiver end. The decision of used precoding matrix can be changed based on precoding information (PCI) feedback from UE. In general there is four possible precoding matrices that provide orthogonality for MIMO transmission. For example, when first stream weights are selected as:

$$w_{1,1} = \frac{1}{\sqrt{2}}, \quad and \quad w_{2,1} \in \left\{ \frac{1+j}{\sqrt{2}}, \frac{1-j}{\sqrt{2}}, \frac{-1+j}{\sqrt{2}}, \frac{-1-j}{\sqrt{2}} \right\}, \tag{4.1}$$

then the weights $w_{1,2}$, $w_{2,2}$ used for second stream are chosen to make columns of precoding matrix orthogonal. The used precoding matrix is signaled to the UE on the HS-SCCH. In MIMO transmission both antennas are transmitting separate pilot signals, so UE can evaluate separate channels based on received pilots [11].

The signaling concerning MIMO transmission information is done in downlink HS-SCCH, that was introduced in Release 5. The channel content and additions brought by MIMO scheme at Release 7 is illustrated in figure 4.2. The channel provides timing and coding information, allowing UE to listen the HS-DSCH at correct time and use the correct codes. HS-SCCH operates with fixed rate 60 kbps, using spreading factor 128. The information in HS-SCCH is divided in two categories. First part contains the physical channel parameters and second part has the control information [11, 33].

The CQI reporting is scheme is different when MIMO is used in HSPA+. Normal CQI mode reports periodically single value between 0 - 30, indicating UE measured channel condition based on pilot signal. When MIMO is used, rank 2 CQI is reported for both streams, based on two different pilots. The CQI values for different MIMO streams range

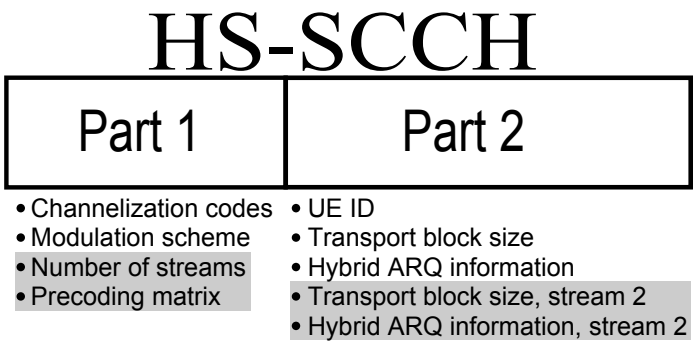

Figure 4.2: *Contents of HS-SCCH. Grey shaded area is only used in when MIMO feature, added in Release 7, is enabled.*

from 0 - 14.

4.3 HSPA+ performance

There are many factors affecting the performance of HSPA+ supporting cell. The UE category class is defining the maximum transfer rates for the device. The features used in NodeB and Radio Network Controller (RNC) also contribute to peak rates, user scheduling and such. The biggest affecting factors, however, are wireless link quality and amount of active users. Even with single user in a cell, if radio link is poor, the peak performance rates can not be experienced. Correspondingly, if the radio link quality is excellent, but the cell is serving lots of users, the capacity and transfer rates for single user are moderate at best.

The schemes used in HSPA and HSPA+ for increasing performance are straightforward in terms of increased peak rates. Higher order modulation use increases the amount of bits used in a symbol. From 16-QAM to 64-QAM, the increase is from 4 bits to 6 bits, translating straight to 50% increase in throughput. Likewise, using schemes like MIMO or dual-carrier gives 100% increase in peak data rates by allowing the use of two simultaneous transport blocks.

Actual throughput for HSDPA physical layer transfer is determined by used modulation, coding rate, transport block size and number of channelization codes in use. These values can change in every 2 ms TTI and are chosen by NodeB, based on channel quality, user scheduling and available capacity for HSDPA. Peak throughput, ignoring maximum transport block sizes, can be calculated as:

$$\textit{Throughput} = \frac{Chip\ rate}{SF} \cdot \textit{Bits per symbol} \cdot \textit{Coding rate} \cdot \textit{Number of codes}, \qquad (4.2)$$

where $Chip\,rate$ is fixed at 3.84 Mcps and spreading factor SF is fixed at 16. Modulation order determines $Bits\ per\ symbol$ value, its is 2 for QPSK, 4 for 16-QAM and 6 bits per symbol for 64-QAM. The $Coding\ rate$ implicates the ratio of information bits in

transmission block. Maximum coding rate is 1, meaning all bits are information bits and no redundancy or error correction bits are used. Coding rate 0.5 means that half of the data bits are information bits and other half are redundant bits that are result of coding [33].

Using equation 4.2 with values corresponding for UE category 10 device, with 15 codes, 16-QAM modulation and coding rate 1, we can get the maximum throughput value of 14.4 Mbps, that is used in for advertising maximum throughputs by network operators and mobile broadband modem vendors. In practice, however, the category 10 device is supporting maximum transport block size of 27952, allowing maximum throughput of 13.976 Mbps with 2 ms TTI, when considering maximum supported coding rate of 0.97 [33]. Release 7 based MIMO capable UEs are in category 15 & 16. With category 16 UE, the practical peak throughput is 27.952 Mbps. This can be obtained when using 2 transport blocks with maximum size of 27952 bits per TTI, 16-QAM modulation, 15 channelization codes and maximum coding rate of 0.97 for each stream, with full transmit data buffer and 100% scheduling for a single user in a cell.

5. LTE

LTE is a term used for next generation wireless radio system designed to offer improvements over 3G network performance. The main aims for LTE is to improve peak user throughput, decrease latency and improve spectral efficiency over HSPA. First LTE specification was finalized in 3GPP release 8 in 2008. The first steps of commercial LTE network implementations have recently begun in several countries, and the number of network providers testing and investing in LTE systems is growing.

The term 4G is often used with LTE technology, although current version of LTE does not yet fulfill the International Telecommunication Union Radiocommunication Sector (ITU-R) 4G requirements for data rates with low mobility communication. The biggest difference in LTE compared to 3G is the new radio access technique, dynamic bandwidth allocation and purely Internet Protocol (IP) based core network. The radio access scheme used in LTE downlink is Orthogonal Frequency Division Multiple Access (OFDMA). LTE uplink direction uses Single Carrier Frequency Division Multiple Access (SC-FDMA).

5.1 LTE basics

OFDMA based radio access principle, used in LTE downlink, is to utilize multiple narrow and mutually orthogonal sub-carriers to transmit desired data. The main concept of OFDMA transmission is to use Discrete Fourier Transforms to move modulated signals between time and frequency domain representation to obtain digital data processing capabilities and provide orthogonality. The orthogonality means that the sub-carrier interference to other sub-carriers is zero and guard bands are thus not required. This allows simpler design of transmitter and receiver. However, accurate frequency synchronization between transmitter and receiver is required in order to maintain orthogonality [1].

Cyclic prefix is added to each symbol in order to avoid inter-symbol interference. This is achieved, when cyclic prefix length is longer than channel impulse response time, then the effect of previous symbol can be removed by discarding the cyclic prefix at the receiver. Cyclic prefix, also called guard interval, eliminates the need to use pulse-shaping filters and reduces sensitivity to time synchronization issues. In LTE, the sub-carrier spacing is fixed to 15 kHz, corresponding to symbol rate of $\frac{1}{15 \quad kHz} = 66.7\mu s$. The supported channel bandwidths chosen for LTE are 1.4, 3, 5, 10, 15 and 20 MHz, allowing more scalability to choose desired bandwidth for LTE systems. Cyclic prefix length is set to be $5.21\mu s$ for first symbol in a time slot and $4.69\mu s$ for the following symbols. Alternatively, extended cyclic prefix with duration of $16.6\mu s$ can be used, in cases of very long channel impulse

response delays. Figure 5.1 shows basic concept of OFDMA transmitter and receiver pair [1, 34, 35].

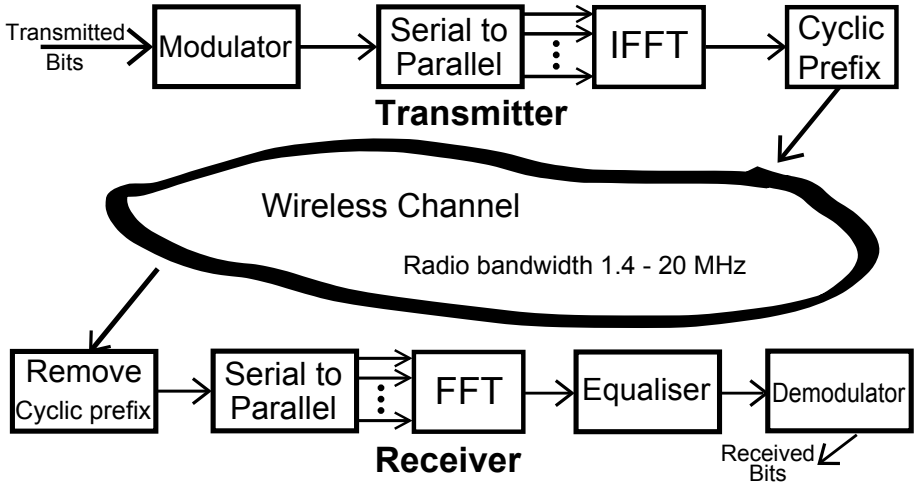

Figure 5.1: *OFDMA transmitter and receiver.*

The uplink scheme in LTE uses SC-FDMA in both TDD and FDD operating modes. OFDMA access is not suitable for uplink direction because of limitations of power amplifier performance in mobile devices. SC-FDMA scheme has better peak-to-average power ratio (PAPR) properties, allowing better uplink coverage and simpler power amplifier design compared to OFDMA. Signal processing of SC-FDMA is still similar to OFDMA, so downlink and uplink parametrization can be harmonized.

LTE resource allocation is done at 1 ms resolution rate for both downlink and uplink. The amount of allocated radio resources per user is distributed in a group of 12 sub-carriers equaling 180 kHz resource block. This resource block is smallest radio resource unit and number of possible resource blocks is dependent of available bandwidth. Transmission bandwidth in LTE is 90% of channel bandwidth. This equals a capacity of 100 resource block for 20 MHz channel bandwidth, 50 resource blocks for 10 MHz and so on, except for 1.4 MHz bandwidth, that only supports 6 resource blocks [1].

One resource block corresponds to one 0.5 ms slot in time domain. One time slot contains 7 OFDM symbols with normal cyclic prefix. One of these symbols is used for reference signals. One subframe, used for resource allocation in time domain, contains two time slots, thus having 14 OFDM symbols. Figure 5.2 illustrates FDD type frame setup for LTE with normal cyclic prefix.

Type 2 frame is used in TDD mode, and it consists of 10 ms radio frame divided in 2 half-frames. Half-frames are further split into 1 ms long subframes. Subframe can be standard subframe used in downlink or uplink, or it can be a special subframe consisting of three fields. These are downlink pilot time slot, followed by guard period and then uplink pilot time slot. The field durations can be configured, but total length of the three fields must be 1 ms.

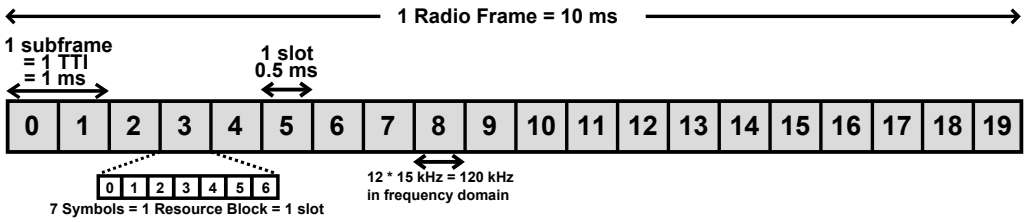

Figure 5.2: *Type 1 Frame for LTE resource allocation.*

Special subframe is used when transitioning from downlink to uplink configuration in LTE TDD mode. Both half-frames always begin with downlink mode. Different configuration parameters determine the amount of subframes used in uplink mode after transition from downlink mode. Each type 2 radio frame contains 1 or 2 transition from donwlink to uplink.

5.2 LTE performance and capacity

The LTE performance is typically measured in cell throughput in user point of view. The cell capacity in LTE is dependent of used bandwidth. It determines the amount of resource blocks that can be scheduled to the users. Figure 5.3 illustrates the relationship of time and frequency domain usage in physical downlink transfer. The allocated units for LTE users are resource blocks, that are built from resource elements.

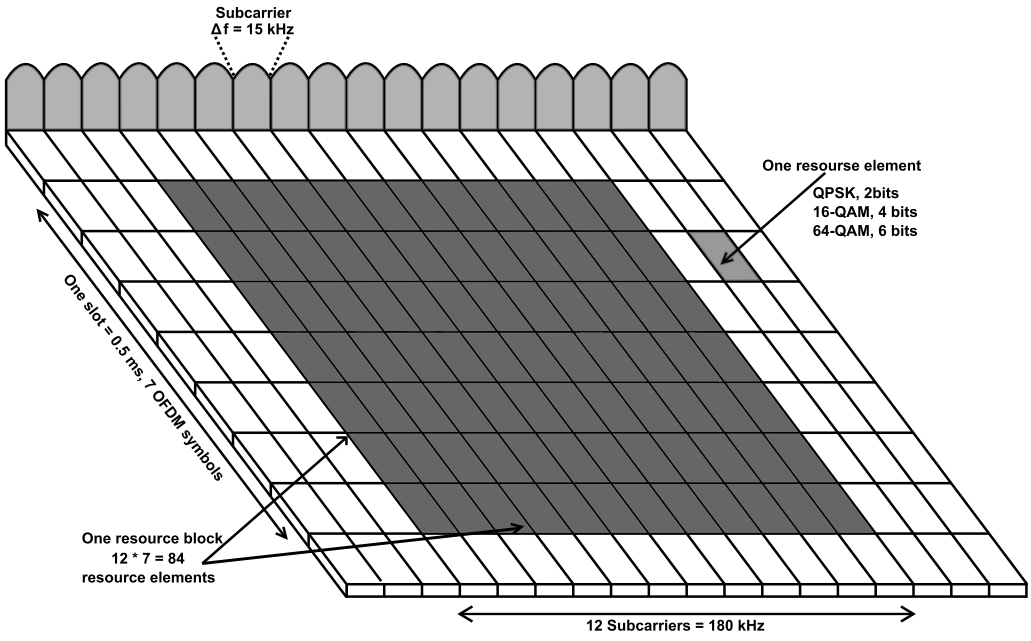

Figure 5.3: *LTE downlink physical elements.*

The theoretical data transfer throughput per second in LTE downlink radio layer can

be calculated as:

$$\textit{Throughput} = N_{RB} \cdot \textit{84 RE} \cdot \textit{Bits per symbol} \cdot \frac{1}{0.5\ ms} \cdot \textit{Coding rate}, \quad (5.1)$$

where N_{RB} is the amount of usable resource blocks, $84\ RE$ is number of resource elements in a resource block and $Bits\ per\ symbol$ is depending on the modulation used in OFDMA symbols. One time slot time is 0.5 ms, 1 is divided by it, in order to get amount of transferred resource blocks per second. Coding rate is the ratio between information bits and redundant coding bits.

When physical channels causing overhead, such as dedicated reference signals, control signals, broadcast and synchronization channels are not taken into account, and no coding is used, the maximum throughput for 20 MHz LTE downlink using 100 resource blocks with 64-QAM modulation, equals to: $100 \cdot 84 \cdot 6\ bits \cdot \frac{1}{0.5\ ms} \cdot 1 = 100.8 Mb/s$. This theoretical maximum rate is not possible to achieve using realistic LTE specific parameters and setup, however it gives an estimate how much capacity on ideal radio conditions LTE based system can handle.

Realistic performance of LTE system can be estimated, by taking into account supported coding rates, transport block sizes and overheads caused by necessary signaling. LTE UE periodically reports CQI values, based on channel conditions estimated from reference signals, to eNodeB. In LTE, the CQI report is between 0 and 15, where 15 indicates best channel quality and 0 report indicates out of serving range. Based on CQI report, BLER target and UE CQI compensation, the Modulation Coding Scheme (MCS), affecting the coding rate and transport block size is decided by eNodeB [36].

MCS parameter range is from 0 to 28, where 28 indicates the biggest transmit block size and coding rate to be used. Based on MSC reported value, UE knows the used transmit block size and coding rate in downlink. With 100 resource blocks and 28 reported MCS, transport block size is 75376. This equals to 75.376 Mb/s transfer rates with a single data stream. For 10 MHz bandwith with 50 resource blocks, the maximum transport block size is 36696, equaling 36.696 Mb/s transfer rate for a single user. With spatial multiplexing MIMO, the amount of data streams, and thus transmit blocks can be increased [36, 37].

Reference signals cause overhead based on how many parallel MIMO streams is used. With 1 stream, the reference signal overhead is approximately 4.8%. With 2 MIMO streams the overhead is 9.52%, and with 4 MIMO streams, the overhead is 14.3%. Reference signal is sent in every resource block at each time slot. Reference signals occupy 4 resource elements in each resource block for one stream, and when using multiple parallel streams, the same resource elements can not be used at the same time, thus increasing the overhead [36, 1].

In addition, the LTE control information signals, using Physical Downlink Control Channel (PDCCH), reserve from 1 to 3 OFDM symbols per subframe when used, causing control signal overhead of 4.8%, 11.9% or 19.0% of cell downlink capacity with normal cyclic prefix. Extended cyclic prefix further increases the PDCCH overhead. In case of

1.4MHz bandwidth, amount of PDCCH symbols is from 2 to 4, incraesing maximum overhead to 26.2%. The used amount of control signaling is dependent of eNodeB configuration and should be based on the amount of users in a cell, and the used bandwidth [36].

The Broadcast channel has 72 subcarriers in OFDMA symbol dedicated to it and uses 4 OFDMA symbols in time slot 1, causing overhead of 0.16% - 2.62%, based on used bandwidth. Synchronization channels use 2 OFDM symbols on every radio frame causing overhead between 0.09% - 1.43%, also based on used bandwidth. Both of these physical channels use fixed amount of resource elements, regardless of used bandwidth. This is why larger LTE bandwidths have slightly less total overhead from physical channels other than Downlink Shared Channel (PDSCH), used for transmit user data [36, 1].

When taking into account all the mentioned overheads, signaling and using coding rate of 0.93, the practical peak throughput rates that can be achieved with optimal channel conditions, such as high received reference signal power (RSRP) and low interference levels, are given in table 5.1. These values are calculated using parameters from LTE

Table 5.1: *Practical LTE peak PDSCH throughput rates (Mbits/sec).*

	Channel Bandwidth					
Antenna setup	1.4 MHz	3 MHz	5 MHz	10 MHz	15 MHz	20 MHz
1 x 1	3.68	11.01	19.29	40.20	60.96	82.05
2 x 2	7.02	20.99	36.75	76.61	116.17	156.35
4 x 4	13.33	39.87	69.83	145.54	220.67	297.02

specifications. The number of PDCCH symbols per subframe used in these calculations is 2. As can been seen from table, the practical peak rates are higher, than maximum transport block size defined by 3GPP standard. Also different UE categories have limitations, how many bits can be received within a TTI. Maximum transport block size is the main limitation for achievable throughput rates for a single user, when channel conditions are optimal.

5.3 LTE with MIMO

The MIMO concept in LTE is similar to HSPA+ implementation. It utilizes spatial multiplexing, precoding and transmit diversity gain. SM utilizes transmitting simultaneous parallel data streams from multiple antennas. In case of LTE standard, 2 x 2 and 4 x 4 MIMO is supported. And even higher level SM schemes, such as 8 x 4 or 8 x 8, are proposed in future releases. Precoding is used to weight parallel signal streams before transmit antenna to maximize the SNR and minimize the correlation between streams. OFDMA access mode used in LTE is well suited for MIMO scheme, because OFDMA can provide locally high SNR that is necessary for SM to work properly [1].

LTE supports several different transmission modes depending on BTS setup and number of Tx antennas. Simplest case is single antenna transmission, where no MIMO or

precoding is used. Transmit diversity can be used when using multiple antennas, without precoding or SM. When open-loop SM MIMO is used, no feedback is required from UE. Closed-loop SM requires the UE feedback, in order to decide the used precoding matrix. Multi-user MIMO allows assigning more than one UE to same resource block, but is not using SM. Closed-loop precoding can also be used without SM transmission. Then it utilizes UE feedbacks for weighting single data streams based on channel properties. Beamforming mode allows to direct the radio wave beam from specific antenna towards determined user location [38].

Parallel data streams in SM MIMO setup are separated into different codewords. Separated codewords use separate scrambling and modulation mapping. When channel conditions are good, both codewords are used for single MIMO capable user, but in case of poor channel quality, second codeword, and thus second data stream can be dropped. Also in case of multi-user MIMO, different codewords are sent to different users. 2 x 2 MIMO can use 2 codewords and 4 x 4 MIMO setup can handle up to 4 separate codewords.

6. MEASUREMENT PLAN

The focus of the performed measurements is to get empirical analysis of the performance of MIMO implementation for HSPA+ and LTE in indoor environment. The fair comparison of performance between HSPA+ and LTE can be achieved, when using same site, antenna configuration and tools for different test cases. The main measurement focus is to study air interface performance of different indoor MIMO setups by means of achieved throughput for a single user. Throughput is used as performance measure because key parameters, depending on MIMO performance and indoor environment effects, are directly affecting the achieved throughput.

6.1 Measurement tools and methods

The software for recording measurement data and performing post-measurement analysis is Nemo Outdoor 5, version 5.81.8 by Anite Finland Ltd. Nemo Outdoor allows to decode, record and view all the parameters, signaling and data traffic between UE and BTS. It also allows easy presentation of the desired values and parameters in real-time using different types of charts and graphs. For advanced data analysis, the measurement files can be loaded to Microsoft Excel by using specific macros to read Nemo log files into Excel sheets. Nemo scripts allow controlling and monitoring the UE behavior and to perform desired operations such as, voice calls, ftp file transfers and PDP initialization.

Flexi Base Station platform by NSN is used as NodeB (for HSPA+) and eNodeB (for LTE) to provide BTS functionality. The software versions used in NSN Flexi Base Stations in the measurements are at the time latest stable performing releases RU20 and RL20. Both software releases are having support for features introduced in 3GPP Release 7, and Release 8 for HSPA+ and LTE.

Indoor antennas used in measurements are Kathrein Indoor Multi-band Directional Antennas, shown in figure 6.1. Antenna element comes with with vertical / dual polarization antennas. (Type No. 80010677). Antenna frequency range for slanted polarization is 1710 - 2700 MHz and gain is 2×7 dBi. Impedance is 50 Ω and VSWR < 2.0. Half-power beam width is 90°, isolation between ports > 25 dB, maximum power 50 W, and protection class is IP 30.

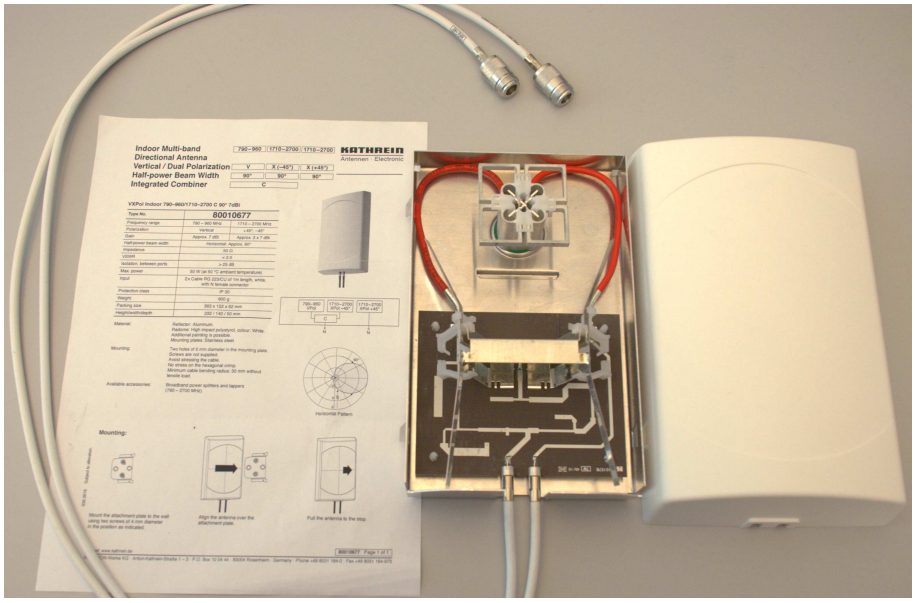

Figure 6.1: *Kathrein indoor directional antenna.*

Novatel Ovation MC996D HSPA+ USB Modem is used in 3G HSPA+ measurements. It is supporting 3GPP Release 99 for GSM/GPRS and Release 7 for HSPA+. Supported bands are 900 and 2100 MHz for UMTS and Quad-band for EDGE/GPRS. HSPA+ UE category class is 18, supporting MIMO with 16-QAM modulation and 0.97 coding rate. Novatel MC996D uses Qualcom MDM 8200 chipset.

The UE used in LTE measurements is commercially available Huawei E398 LTE 4G USB Modem, and it is based on LTE UE category class 3 specifications. Huawei E398 is, in addition to LTE, also supporting GSM-EDGE, 3G HSDPA and HSPA+. Supported LTE frequencies are 800 MHz, 1.8 GHz and 2.6 GHz. The NSN LTE network is set to operate in 2.6 GHz frequency at the time of measurements. Huawei E398 uses Qualcom MDM9200TM chipset, capable of providing triple-mode modem operating capabilities. Novatel MC996D and Huawei E398 USB modems are shown in figure 6.2.

Figure 6.2: *Wireless modems used in measurements. Novatel MC996D modems on right and Huawei E398 modems on the left.*

Throughput performance measurements are conducted by using user datagram proto-

col (UDP) type of transmission. Using local server to continuously feed buffered UPD packets for a single user allows full congestion of network utilization and throughput. This allows full utilization of wireless channel shown in MAC-hs traffic rates. Unlike TCP, UDP does not utilize retransmissions, flow control or error corrections. UDP keeps sending packets at specified rate no matter if they are received or not. Other measurement parameters for analyzing and discussion are performance related parameters like RSCP & RSRP, UE reported CQI values, MIMO utilization percentage, transmission block sizes and used modulations and coding rates.

Using an empty cell and free frequency band ensures minimum possible interference that can affect the measurements. However, the office area measurements can experience small variations due motions and other phenomenons caused by people inside the building. This effect is tried to be kept minimal by averaging the measurements over longer time period, and performing every measurement multiple times, in order to get more reliable results. In LTE setup, 10 MHz bandwidth is used in the measurements because of limitations of UE capabilities. 10 MHz bandwidth allows air interface to be fully utilized for single user and peak rates can be expected with measurement equipment.

Different test cases are conducted using same measurement routes, locations and device setups in order to ensure valid comparison of results. The measurement routes are first and second floor corridors and open areas in Karaportti 1. In addition, stationary measurements are taken in rooms with different distance from transmit antenna. The second floor measurements offer weaker signal strengths due increased attenuation, corresponding to performance experienced at cell edge areas. Mobile measurements are done along the routes by walking slowly, roughly 2 km/h, and pushing the measurement equipment cart table shown in figure 6.3. Stationary measurements are conducted by keeping the UE in a

Figure 6.3: *Mobile measurement equipment cart setup.*

fixed location and slowly rotating it around in order to measure the effect of UE receiver orientation in terms of throughput.

6.2 Measurement environment

Indoor measurements were conducted in NSN office building at Karaportti 1, Espoo, Finland. The antennas were installed in first floor of the Karportti 1 building. At the measurement location, all doors around routes and static locations are kept closed during the measurements. The detailed measurement routes and locations are presented and discussed in the next chapter with results.

The physical connection setup with all used components is shown in figure 6.4, where

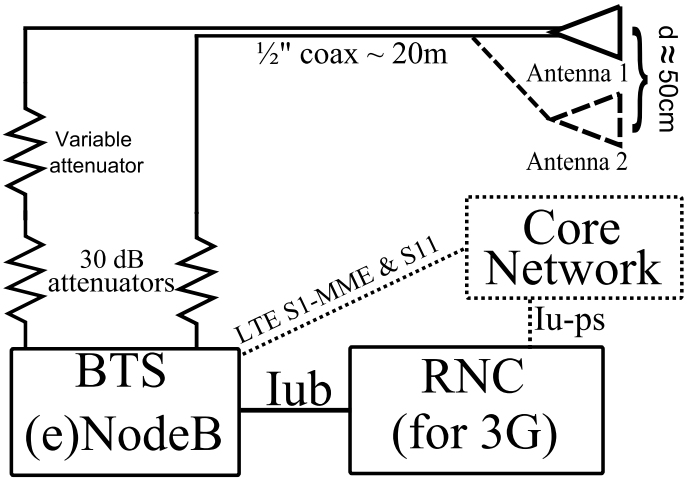

Figure 6.4: *Physical connections between radio access elements.*

antennas and cables are same for both LTE and 3G systems. Cables connecting the antennas to BTS are 1/2" coaxial cables manufactured by Draka NK, and are connected with N-type connectors. Cable losses are given as attenuation in dB/100m at 20° Celsius ambient temperature by the cable manufacturer. For 2100 MHz operating frequency used in 3G system the given cable loss is 16.0 decibels per 100 meters, and for LTE system with 2600 MHz operating frequency the cable loss is 18.0 decibels per 100 meters.

30dB attenuators are used on BTS end to provide sufficient attenuation for desired power levels, in order to limit the cell size close to the measurement area. The BTS that is used for HSPA+ measurements is called NodeB, and for LTE the BTS unit is called eNodeB. The RNC element functionality that is used for 3G UMTS system is implemented into the eNodeB in LTE. Also core network elements after the BTS are different for 3G and LTE.

The 3G NodeB transmission power is set for 20W per antenna line, while LTE eNodeB transmission power is set to 40W for each antenna line. While LTE transmission power is twice as much as the 3G, the higher frequency causes more attenuation in cables, connectors and air interface, making cell coverage area and received power levels in used

test setup very close between 3G and LTE. PDCCH symbols were set to 2 for LTE setup, according to realistic implementation of 10 MHz LTE cell.

6.3 Test cases

The following test cases are studied in the indoor field measurements with HSPA+ and LTE setups.

- Indoor environment effect with MIMO setup.
- Gain of using MIMO compared to case of a single antenna.
- Effect of polarization diversity versus spatial diversity with MIMO.
- Effect of antenna feeder imbalances for different antenna lines.

Multiple measurements, two to three times for each test case, are performed in order to get more reliable and accurate results. Having more measurement data for each case allows possible distortions and anomalies to be discovered and discarded from presented results.

6.3.1 Indoor environment effects with MIMO

The effects of different indoor locations and places are studied with MIMO setup. In this test, the measurement locations and routes are chosen to provide different indoor propagation paths for wireless signals. Both LOS and NLOS cases and effect of distances and slow mobility measurements are studied with wireless indoor channel point of view. This gives analysis base for MIMO setup performance in different indoor locations. This test case is also used to set reference measurement results against other test cases. The antenna setup is using cross-polarization diversity SM MIMO for this case. The cross-polarization antenna setup is chosen as reference, because it has in these measurement cases the simplest MIMO implementation by using only one antenna element with two antenna lines.

6.3.2 MIMO gain

Testing for performance gain provided by MIMO setup is done by measuring and comparing throughputs and other network parameters when MIMO option is disabled. This test case is performed by disabling MIMO from BTS, thus only single data stream block is sent from Tx. When MIMO is not used, HSPA+ UE can support 64-QAM modulation, allowing better throughputs, than 16-QAM, that is used in MIMO enabled case due to limitations of UE support. For more thorough analysis, the measurements are done with both 64-QAM option enabled and disabled for the cases of non-MIMO with HSPA+. LTE UE supports same 64-QAM modulation with and without MIMO transmission.

Additional test case is measured when transmit diversity is used, allowing transmitting single data stream with two antennas, providing double total transmission power and diversity gain. It is expected that the diversity gain and capacity increase from SM provided with MIMO setup should increase both SNR and received power. These benefits are shown with increased throughput and channel quality assessments. With locations that are less suitable for MIMO transmission, the 64-QAM modulation enabled single stream transmission is expected to perform close to SM, or even better in some cases with HSPA+. With LTE setup, the SM MIMO case should always provide best performance. When channel condition is good for SM, the MIMO supported transmission should provide notably better performance against single transmission cases. Also, Tx diversity case is expected to outperform single antenna line setup in all cases, by providing more diversity and twice the transmit power.

6.3.3 Effect of polarization diversity versus spatial diversity with MIMO

The diversity gain and SM can be achieved with both polarization and spatial diversity. In this test case, both antenna setups are measured and compared in order to evaluate if there is differences between these two schemes. Spatial diversity can be measured by adding another antenna next to first antenna, and connecting one feeder to both antennas. Also hybrid case measurement is possible, when another antenna feeder is connected to different polarization than first one. In hybrid case, the MIMO setup provides both spatial and polarization diversity.

The expectation is that spatial diversity case offers similar results as polarization diversity, because both setups are introducing different channel properties for separate streams. The hybrid case with both spatial and polarization diversity should offer best results, because channel correlation is expected to be least in this setup. However, the performance differences between different antenna diversity setups are not expected to be significant.

6.3.4 Effect of antenna feeder imbalances

The effect of imbalance in signal levels on antenna feeders is tested by using attenuator for other antenna cable causing more signal loss for other antenna element. Imbalanced signal is expected to result degradation in performance of MIMO SM efficiency and utilization, because the channel capacity for streams with different attenuation is less. In addition, a stronger stream can cause more interference to the weaker stream, when correlation is experienced. The focus of this test case is to find what imbalance levels start to have notable affect on performance, and what levels make MIMO scheme unusable.

7. RESULTS & ANALYSIS

This chapter focuses on presenting results for each test case in figure formats, allowing visual presentation and easier comparison between different setups. For more thorough analysis, all the throughput results in every test case are presented in Appendix A in a table format. All the results presented in this chapter are gathered averages from several measurement for each case. All anomalies in results are filtered out by discarding those measurements that experience unusual performance rates compared to other measurement runs. The averaging throughputs and other values are obtained from one second time intervals. This one second averaging interval hides the effect of fast fading, and also the absolute maximum and minimum throughput peaks, because those typically happen only during one or few TTI periods.

Throughput values in measurement results are given in a value of megabits per second (Mb/s or Mbps). These throughput values were obtained by UE reported downlink medium access control (MAC) -layer transmission rates, including MAC-layer overheads. MAC-layer throughput rate in wireless data transfer indicates amount of user data transmitted in the air interface between BTS and UE. Throughput values presented in results are divided in specific sections along mobile measurement routes, and specific stationary measurement points for MIMO diversity cases.

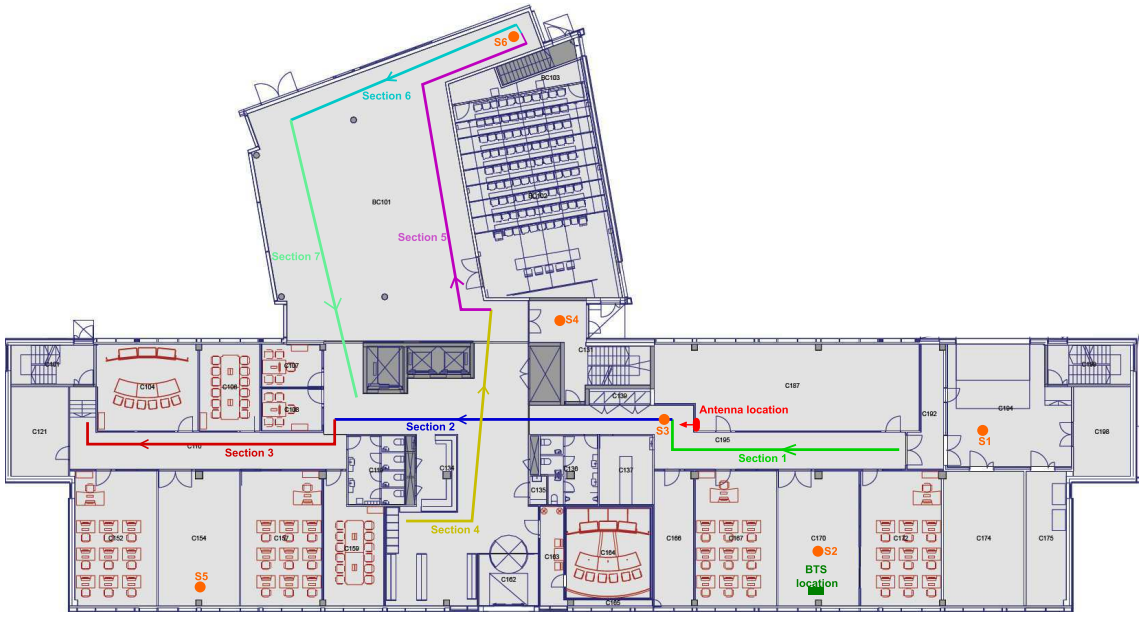

Figure 7.1: *First floor measurement area.*

First floor measurement routes are divided into 7 different sections and second floor route has 4 sections. These sections are chosen to provide different channel conditions within measurement area, so comparison of different test cases can be analyzed more efficiently. Figure 7.1 illustrates 1st floor routes and static measurement spots. Mobile measurement sectors are marked with colored lines with arrows marking the direction of movement. Static spots are marked with orange circles, to present area where static measurements were performed. Antenna location and beam direction is also shown in both figures.

First section begins behind the antenna element and ends up in front of the antenna. Second section goes from front of antenna in LOS to the end of the hallway. Third section goes along the corridor and is still barely LOS situation, where antenna is partly visible along the section. From fourth section till end of fifth section, the motion is perpendicular to antenna directivity. End of fifth section is the weakest reception area in the first floor. Section six and seven go through open space area, ending up to the LOS spot after corner, near the end of section 2.

Figure 7.2 covers the second floor measurement area routes and static spots. Second

Figure 7.2: *Second floor measurement area.*

floor measurements mainly correspond to case of cell edge, based on signal strengths. Section 8 starts in front of the antenna element, one floor below. It goes through corridor and hall area, ending up in front double window doors with heavy metal frames. Section 9 is short, it consist of opening a door, moving through it to other side and waiting door to close. Section 10 leads along a corridor, going away from antenna. End of section 10 has very weak signal levels, and few cell drops were experienced there. Last section 11, goes from hallway area to a corridor connecting to next building.

While all other other route sections are accurately fixed between test cases, the end of the second floor last section measurement was marked when data connection was lost. The spot where connection was lost varied between different measurement runs and test cases, with maximum variation of approximately 5 meters. This makes last section of second floor measurement route less comparable, because the section length is not exact and time measured at the end of section varies, making the section results less compatible against each other. The static spots were chosen to represent different spots around measurement area in terms of obstacles and signal attenuation levels. The purpose of static measurements is to show the range of throughput rate changes in a static location by only changing the orientation of UE.

7.1 Indoor MIMO performance results

This section focuses the performance of reference MIMO measurements using cross-polarization antenna setup with SM scheme. The best throughputs are experienced in first floor sections, near the antenna and on sections with LOS connection. The throughput performance seen in results also has a correspondence experienced channel quality. The big difference between maximum and minimum values indicate that SM MIMO scheme, especially with HSPA+, is very sensitive to channel variations and receiver orientation.

Figure 7.3 shows the measured throughput rate and RSCP levels in first floor sections, and figure 7.4 presents MIMO utilization percentage and UE reported CQI values along

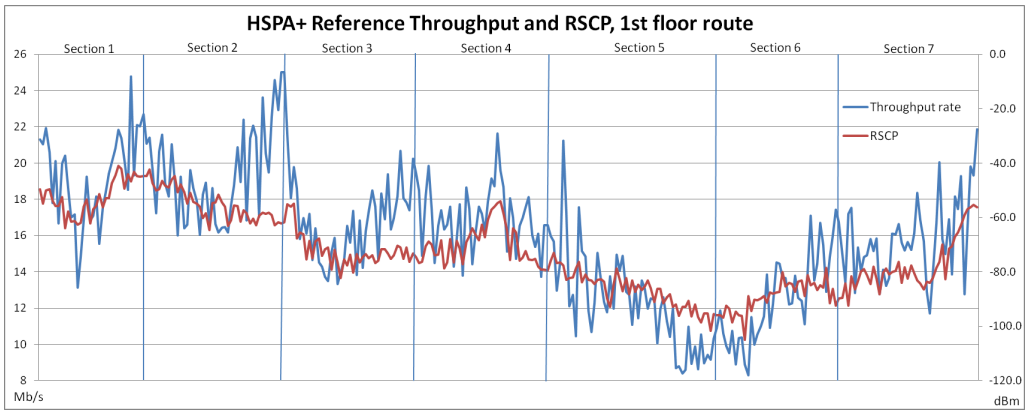

Figure 7.3: *HSPA+ first floor reference throughput.*

the same measurement. From figures 7.3 and 7.4 it can be seen, that with HSPA+, the throughput performance trend follows closely to UE reported CQI values and measured RSCP levels in the first floor sections. Also, notable case with HSPA+ is that second stream CQI values are constantly lower than first stream, meaning that second transmission block size is smaller. This explains why maximum throughput rates are not achieved. MIMO utilization percentage follows closely the CQI levels. With low CQI values, MIMO utilization is also low, meaning that second data stream is sent only part of the time when

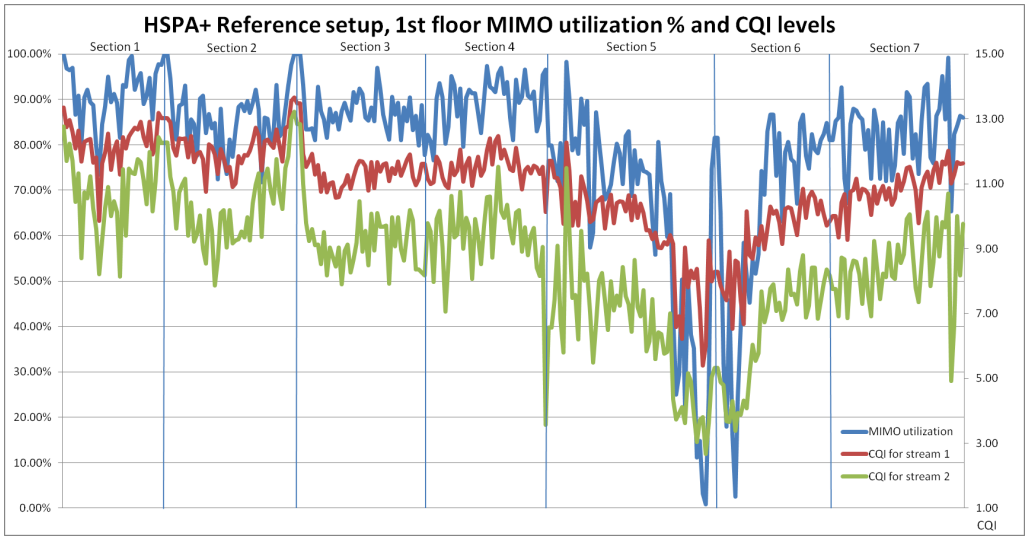

Figure 7.4: *HSPA+ first floor reference RSCP and CQI levels.*

utilization percentage drops. Only bad reception area in first floor is found in between section 5 and section 6.

Figure 7.5 shows the throughput rates and RSCP levels seen in second floor reference mobile measurement, and figure 7.6 presents the MIMO utilization percentage and CQI

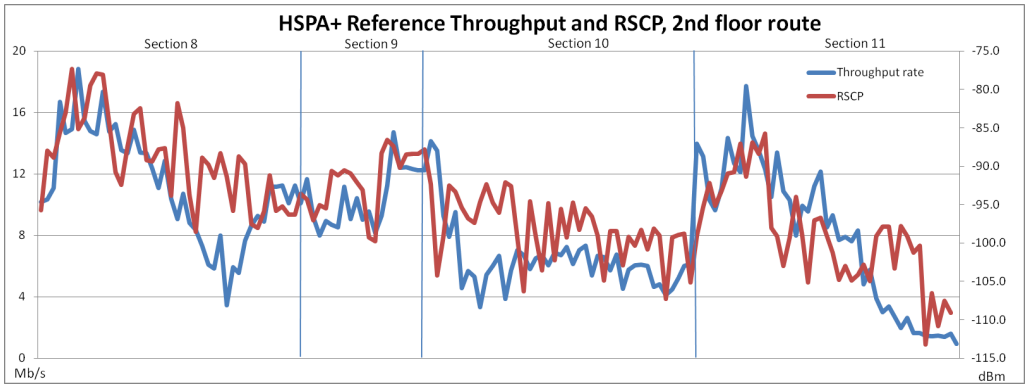

Figure 7.5: *HSPA+ second floor reference throughput.*

levels from same measurements. In second floor results, the throughput rate is still following the RSCP levels, and CQI values share very similar behavior trend as the throughput rate. Also in second floor case, the CQI value difference between streams is similar to the case of first floor and MIMO utilization is somewhat following the CQI levels. The trends in second floor are similar to the first floor case, but the variations are larger. MIMO utilization drops to 0% in worst areas of second floor routes. The performance levels in the second floor are notably lower than in the first floor, except the few peaks experienced near the antenna location.

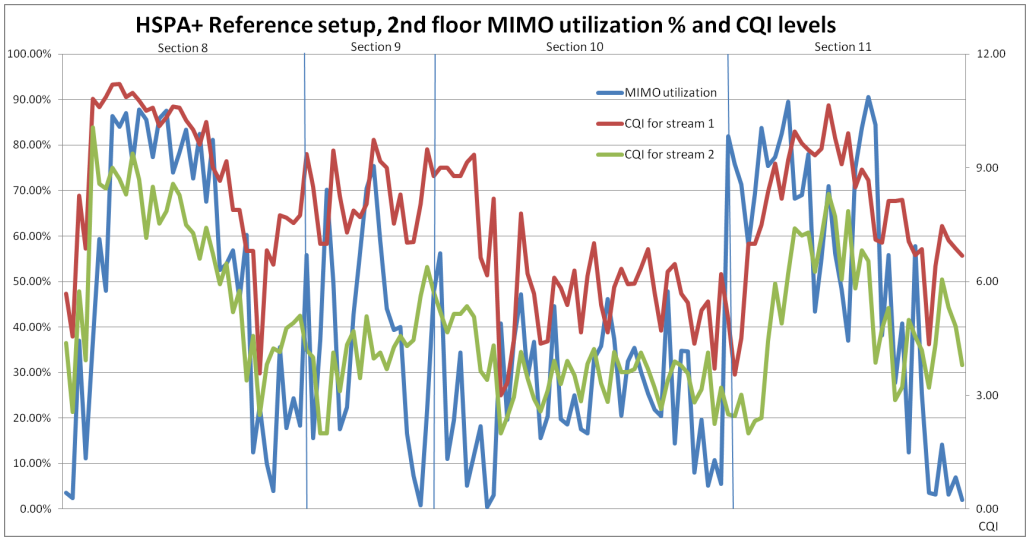

Figure 7.6: *HSPA+ second floor reference RSCP and CQI levels.*

Figure 7.7 shows throughput rates in first floor LTE reference setup measurements, and

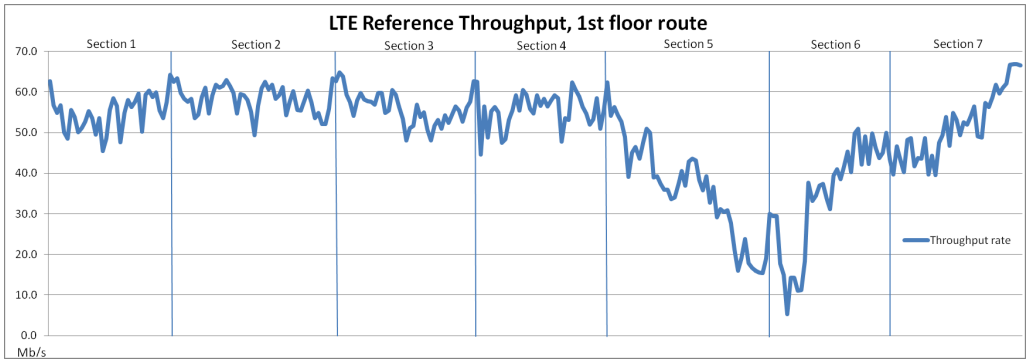

Figure 7.7: *LTE first floor reference throughput.*

figure 7.8 shows the measured RSRP level and reported MCS values for both codewords. As seen in the figure 7.7, the throughput rate with LTE is high in almost whole first floor. Only at the sections 5 and 6 the rate experiences considerable drop, because of bad channel quality. From figure 7.8 it can be seen, that in case of LTE, the throughput rate does not follow the RSRP levels, but it is following the trend of MCS. It suggests, that in good channel conditions, the signal levels do not affect the performance. Also compared to HSPA+ throughput rate, the LTE throughput performance appears to be more stable on good channel conditions. This suggest that OFDMA radio access mode performs better with MIMO reception than WCDMA.

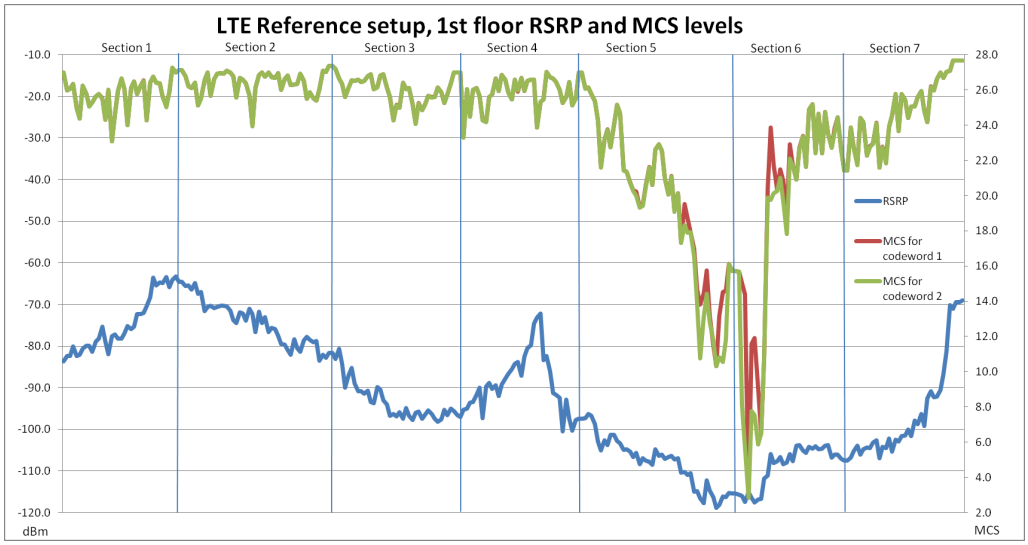

Figure 7.8: *LTE first floor reference RSRP and MCS levels.*

Second floor throughput rates for LTE reference setup are shown in figure 7.9, and figure

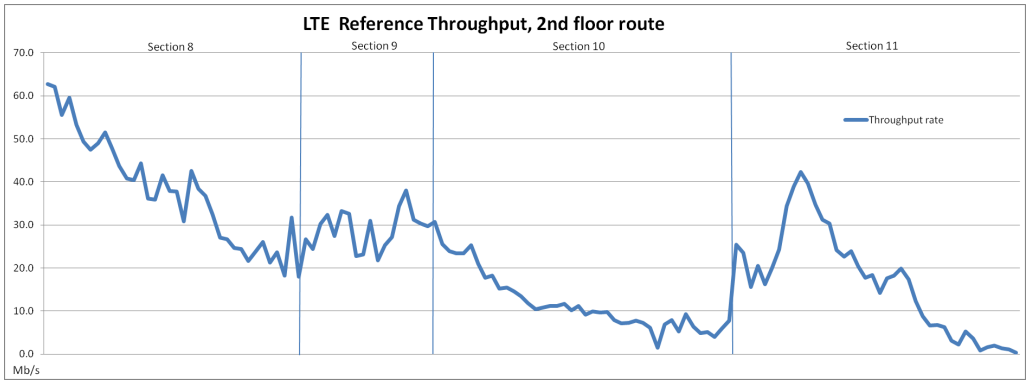

Figure 7.9: *LTE second floor reference throughput.*

7.10 shows measured RSRP levels and MCS values for both codewords. At second floor, where signal attenuation is much greater and amount of strong MPC are less, the LTE rate trend is very similar to HSPA+. Again the throughput rate does not correspond to RSRP levels, but it follows the MCS values. While throughput rate is still considerably high at good reception areas, the rate quickly drops when moving close to cell edge area. On worst channel conditions experienced in second floor, the LTE throughput rates drop to very low values. On these areas, the LTE configuration does not offer any notable improvement compared to HSPA+. The used hardware and software configuration could not display the CQI values, reported by LTE UE, or MIMO utilization percentages. The SM MIMO setup is lost on worse channel conditions, when the MCS for codeword 2 drops to 0. When channel quality improves, the second data stream is sent again.

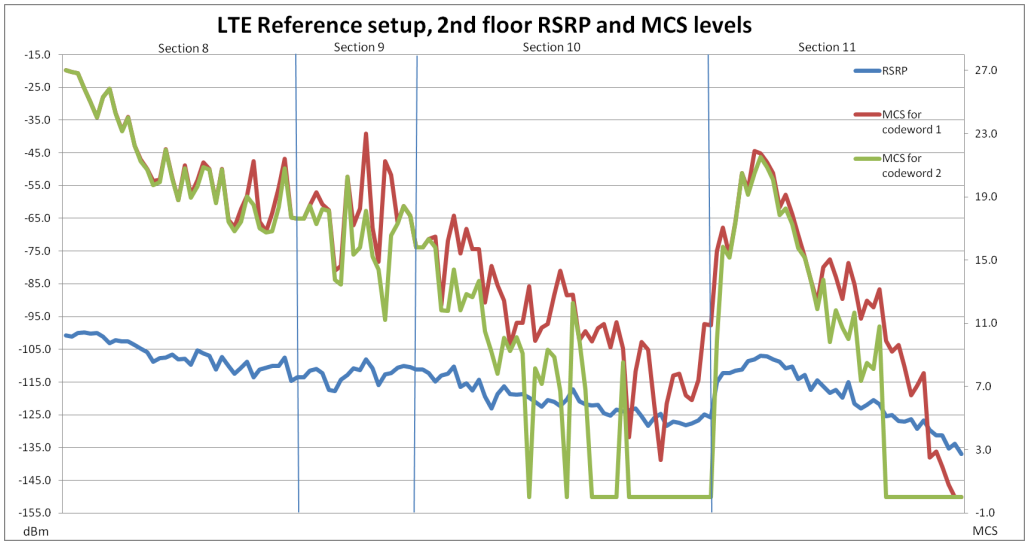

Figure 7.10: *LTE second floor reference RSRP and MCS levels.*

Figure 7.11 illustrates achieved throughput rates from reference static spot measurements for both HSPA+ and LTE. The maximum rates in LTE are considerably higher than in

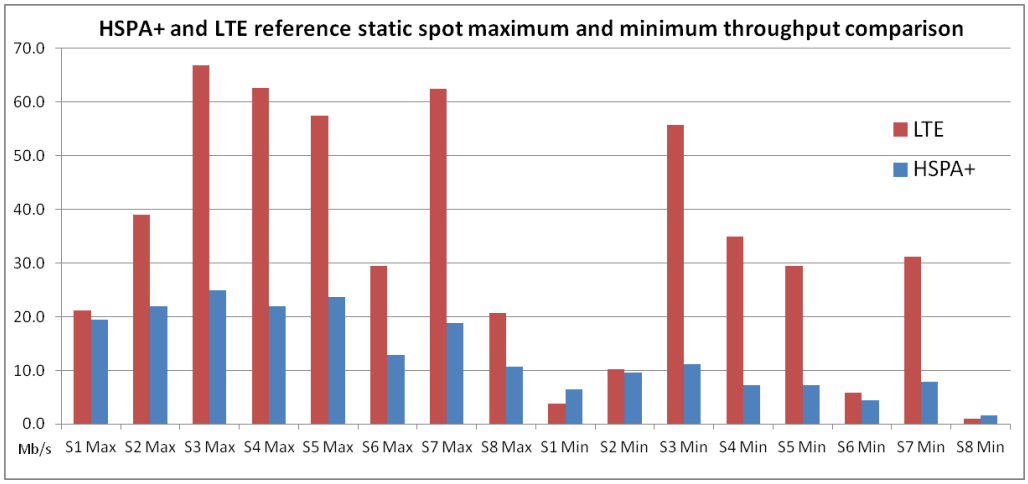

Figure 7.11: *Reference static measurement maximum and minimum rates for HSPA+ and LTE.*

HSPA+ case for most spots. Minimum throughput rates also perform similarly. LTE greatly outperforms HSPA+ minimum rates on good channel quality spots, but at worse locations, the minimum rates are similar for both cases.

When comparing LTE and HSPA+ performance in terms of spectral efficiency, and taking into account that LTE uses double bandwidth and supports higher modulation than current HSPA+ MIMO, the difference becomes less. LTE appears to be slightly more efficient in terms of spectrum utilization on good channel conditions. While on locations with worse channel quality, the spectral efficiency with LTE is similar, or even worse than with HSPA+. The variance between maximum and minimum throughput values varies be-

tween static measurement spots, but the sensitivity of MIMO performance and difference between the peak rates and minimum rates are always large for both HPSA+ and LTE.

7.2 MIMO gain over single antenna setups

MIMO performance is compared against non-SM setup, using only single antenna line, or using 2 antenna lines with transmit diversity MIMO scheme sending only one data stream. For HSPA+ both 64-QAM and 16-QAM measurements were made in single antenna line and Tx diversity MIMO setups.

Figure 7.12 illustrates average throughput comparison between SM MIMO, transmit diversity and single antenna line HSPA+ setups. Average throughput rate comparison give

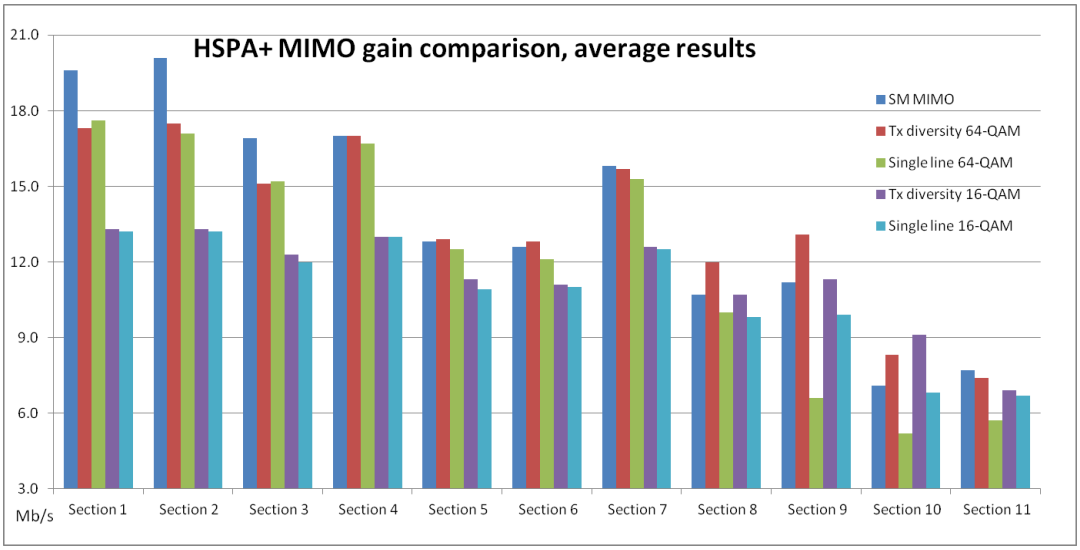

Figure 7.12: *Average throughput comparison with HSPA+ setups.*

best the comparison point for MIMO gain effect. With average results, the SM MIMO outperforms 64-QAM setups in first three sections, that have best channel condition for MIMO. Rest first floor sections the SM MIMO performance is close with 64-QAM setups, and 16-QAM is limited to near maximum rates in whole first floor. Based on difference between 16-QAM and 64-QAM results, it would implicate that HSPA+ SM MIMO would gain more throughput if 64-QAM modulation was supported with two transmit blocks. In the second floor average results the 64-QAM transmit diversity outperforms the SM MIMO. And all the rates are withing few megabytes per second, except the 64-QAM single line setup.

The reason behind poor performance of the 64-QAM single line setup in second floor appears to be increased interference from unknown source. The frequency band used in HSPA+ measurement was scanned to be unused, but measurement logs show that 64-QAM single line setup experienced on average 3dB lower Ec/No levels and reported lower CQI values than other second floor measurement. No other HSPA+ measurement experienced this interference.

Figure 7.13 presents maximum throughput comparison between SM MIMO, transmit diversity and single antenna line HSPA+ setups. As seen from figure 7.13, the maximum

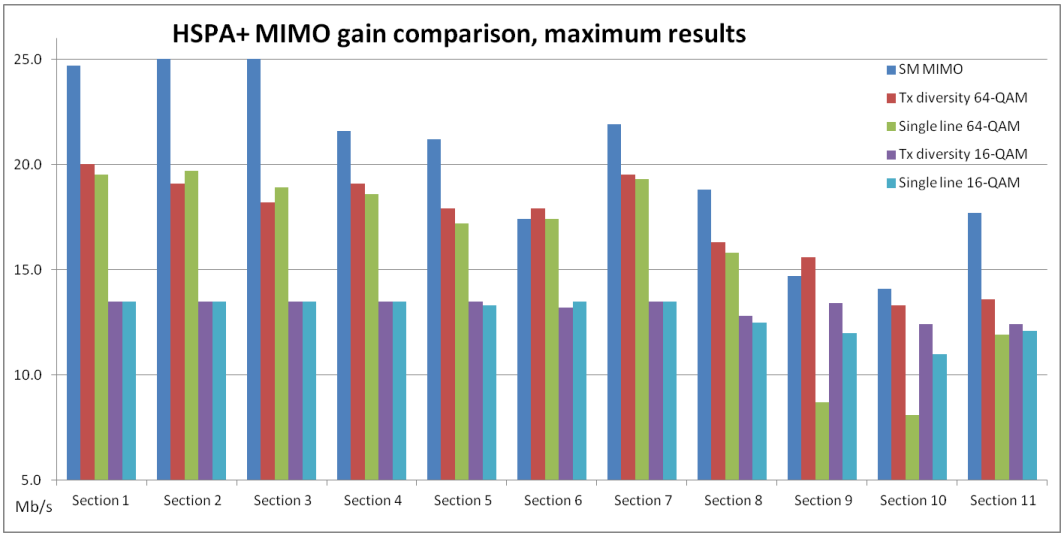

Figure 7.13: *Maximum throughput comparison with HSPA+ setups*

throughput rates are achieved with SM MIMO configuration in most of the sections. The transmit diversity does not provide notable benefit in maximum rates for 64-QAM or 16-QAM setup in first floor sections, but in the second floor the transmit diversity gain is more clearly seen. Noticeable anomaly is again the 64-QAM single line performance in the second floor sections. The maximum rates are notably lower in sections 9 and 10, than any other setup.

Figure 7.14 presents minimum throughput comparison between SM MIMO, transmit diversity and single antenna line HSPA+ setups. The minimum rates between different

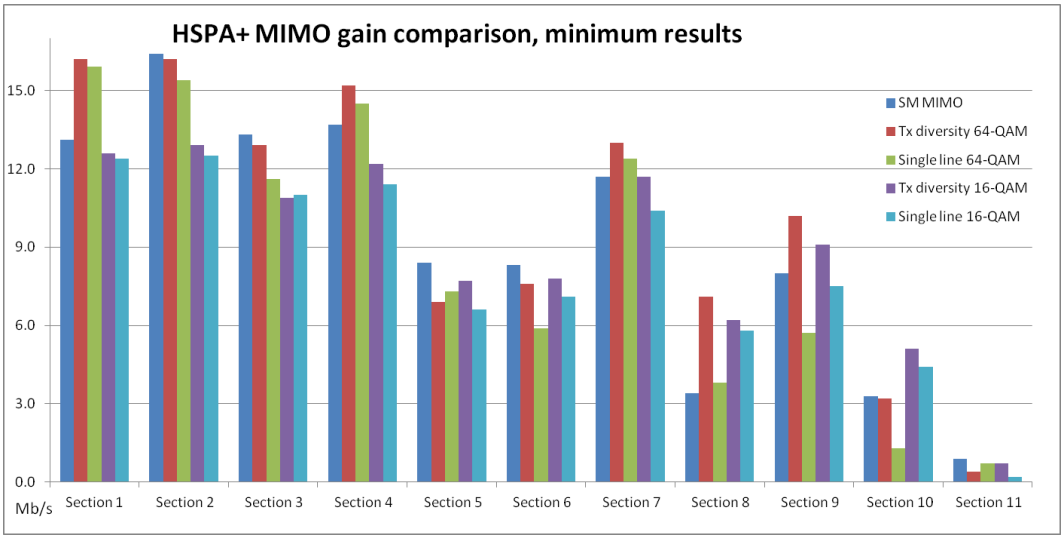

Figure 7.14: *Minimum throughput comparison with HSPA+ setups.*

setups are all close to each other. This result is expected, as when worst channel quality is

experienced in each section, all the setups use similar link adaptation scheme, 16-QAM or QPSK modulation and single data stream. The 64-QAM setups have best minimum rates in some sections, implying that sensitivity of SM MIMO experiences high variations in throughput, showing in high top peaks and low minimum rates. Also with minimum rates, the single line 64-QAM setup is performing poorly in second floor sections.

Figure 7.15 illustrates average throughput comparison between SM MIMO, transmit diversity and single antenna line LTE setups. It can be seen from figure 7.15, that the

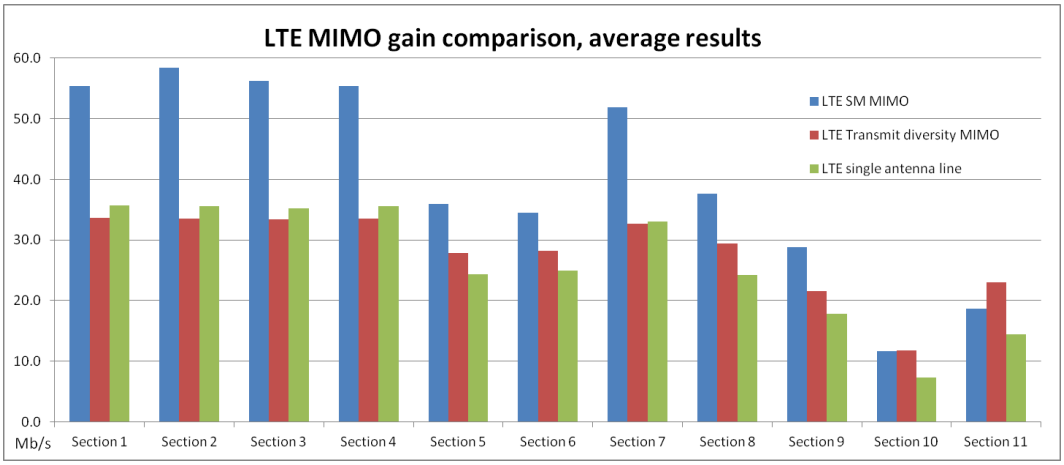

Figure 7.15: *Average throughput comparison with LTE setups.*

SM MIMO is performing noticeably better than other two, except in second floor worst sections, where MIMO utilization is low. Single antenna line case outperforms transmit diversity MIMO in first four sections. Reason behind this is that transmit diversity has more overhead in terms double amount of reference signals when using two transmit antennas, increasing overhead by nearly 5%.

Figure 7.16 illustrates maximum throughput comparison between SM MIMO, transmit

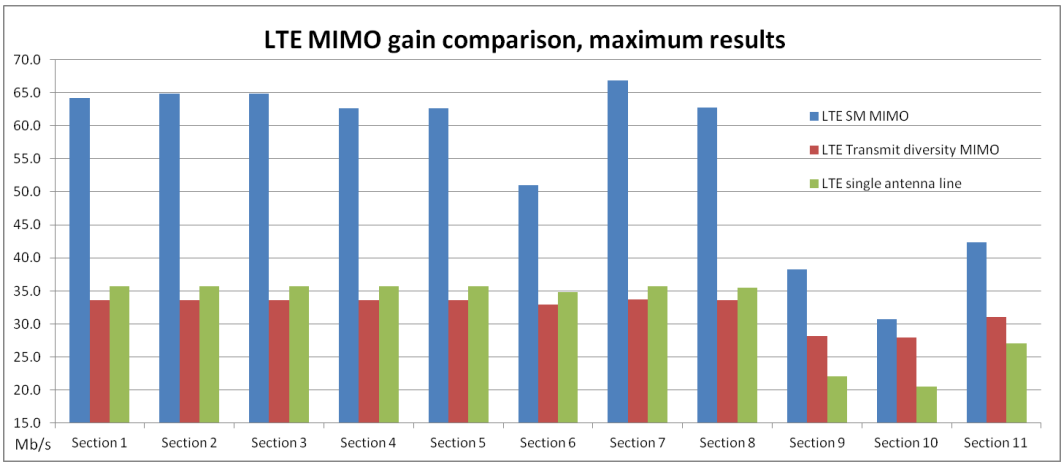

Figure 7.16: *Maximum throughput comparison with LTE setups*

diversity and single antenna line LTE setups, and figure 7.17 shows same comparison with

minimum measured throughputs. With maximum results, the open loop SM MIMO setup

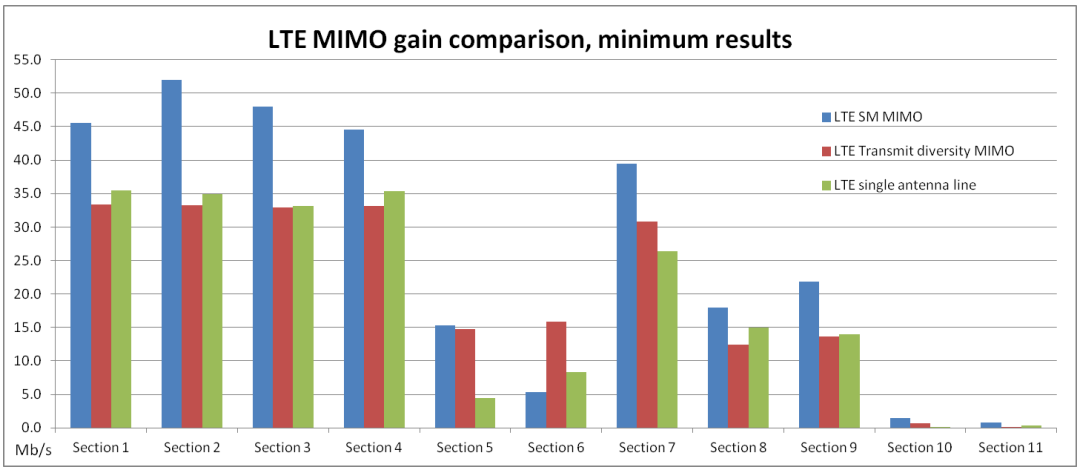

Figure 7.17: *Minimum throughput comparison with LTE setups.*

clearly outperforms the single line and transmit diversity setups in every section. The interesting notice is that on sections with good channel condition, the single line setup constantly outperforms the transmit diversity setup. Only on second floor sections with worse channel quality, the transmit diversity gain against single line shows as increased maximum throughput.

As in the case of maximum throughputs, also in minimum throughputs the SM MIMO is performing best, except in section 6. Also case with single line and transmit diversity setup is similar where single line is better in sections with better channel quality, while transmit diversity gain shows in sections that have worse channel quality.

Overall, the LTE results are clearly indicating that SM MIMO mode, in cases where channel condition allows proper MIMO utilization, clearly offers best throughput rates in all terms from minimum to maximum rate. With the HSPA+ case, the results and gain of MIMO setup was not so clear. These results further imply that MIMO with OFDMA seems to be more robust to sensitivity than WCDMA. Only drawback LTE has is the relatively poor performance at cell edge areas.

7.3 Antenna diversity setup comparison with SM MIMO

Performance of different MIMO antenna setups are compared and analyzed. Polarization diversity is the reference case when antenna unit has two cross-polarized transmit antennas. Spatial diversity is obtained by placing two of these antenna units apart and connecting the antenna lines with same polarization. Hybrid diversity case is combining spatial diversity and polarization by connecting separate antenna units with separate polarization lines.

Figure 7.18 presents the average mobile section throughputs for different antenna diversity case. With average rate comparison, the differences between diversity performance

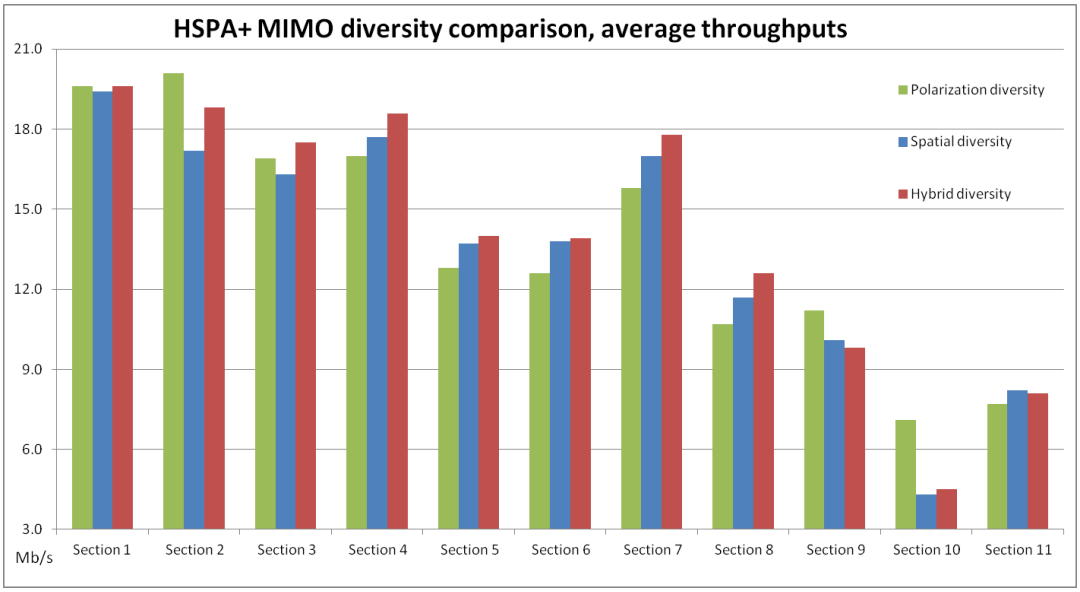

Figure 7.18: *HSPA+ antenna diversity comparison, average results.*

are generally small. No diversity scheme appears to be dominant, or provide notable gains over other setups in average rates. Only in the second floor section 10, the polarization diversity notably performs the other two.

Figure 7.19 presents results of maximum achieved throughputs for HPSA+ with different diversity cases, and figure 7.20 shows the minimum throughput rates with same

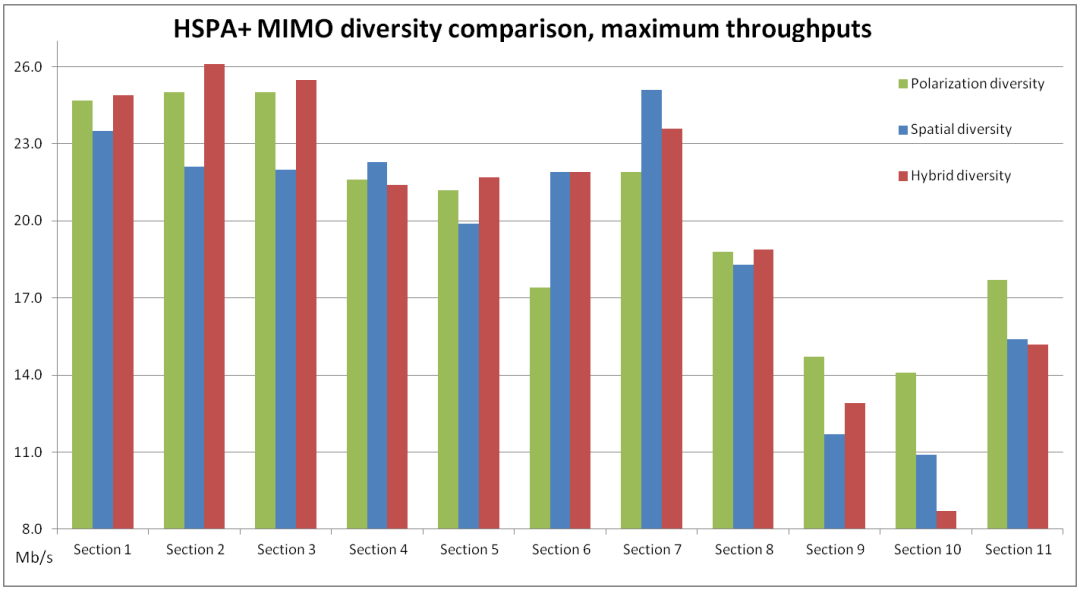

Figure 7.19: *HSPA+ antenna diversity comparison, maximum results.*

measurement configurations. With maximum results, the first three sections in first floor having mostly LOS connection, it appears that polarization and hybrid diversity cases offer better maximum peaks than spatial diversity. Rest of the first floor sections are more

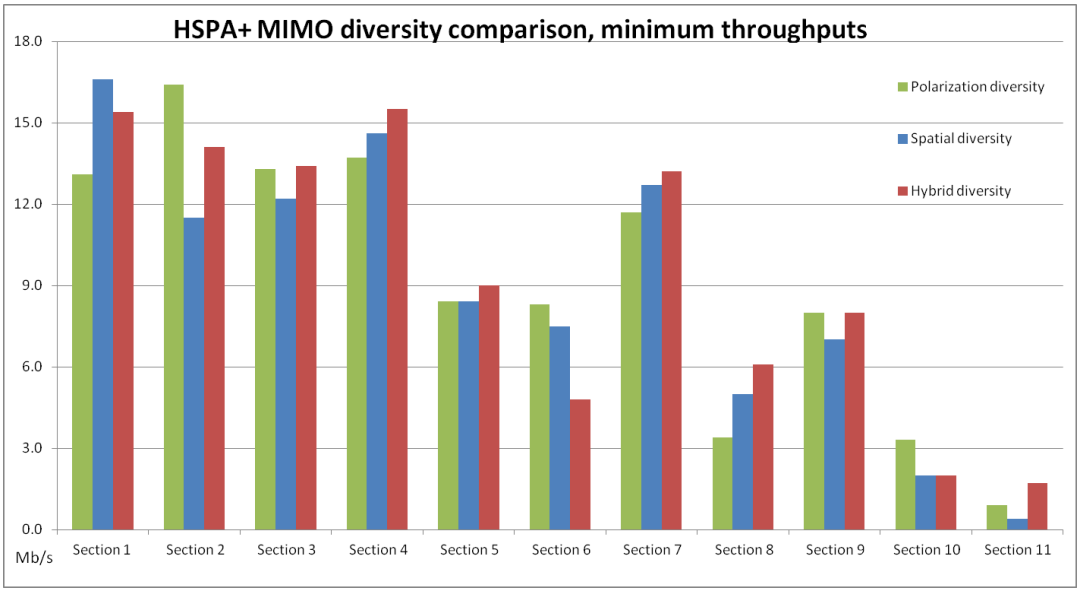

Figure 7.20: *HSPA+ antenna diversity comparison, minimum results.*

even, except on section six, where polarization diversity peak rate is notably less than others. On second floor sections the polarization diversity seems to outperform other two in maximum rates. Reason for this might be that the spatial distance between antennas experience different attenuation rate when penetrating the ceiling between first and second floor.

The minimum rates seen in figure 7.19 are similar to maximum rates. No diversity scheme appears to be notably better or worse than other. Each setup has best and worst rates depending on the section. For worst sections in first and second floor, the SM MIMO usage is close to 0% in case of these minimum results. This makes minimum rate comparison less valid than maximum or average throughput rate, because diversity scheme gain only affects the reception of single data stream.

Overall, these results suggest that HSPA+ SM MIMO scheme works in indoor environment with any type of antenna diversity setup. The polarization diversity antenna setup can be recommended, because it has easiest installation with only one antenna unit. Based on all the results, the spatial diversity setup with HSPA+ is performing worse than other two by a slight margin.

Figure 7.21 shows the HSPA+ maximum and minimum static throughput results with different diversity setups.The static result comparison with different diversity scheme is studying if any antenna diversity setup has clear advantage for MIMO reception in static locations.

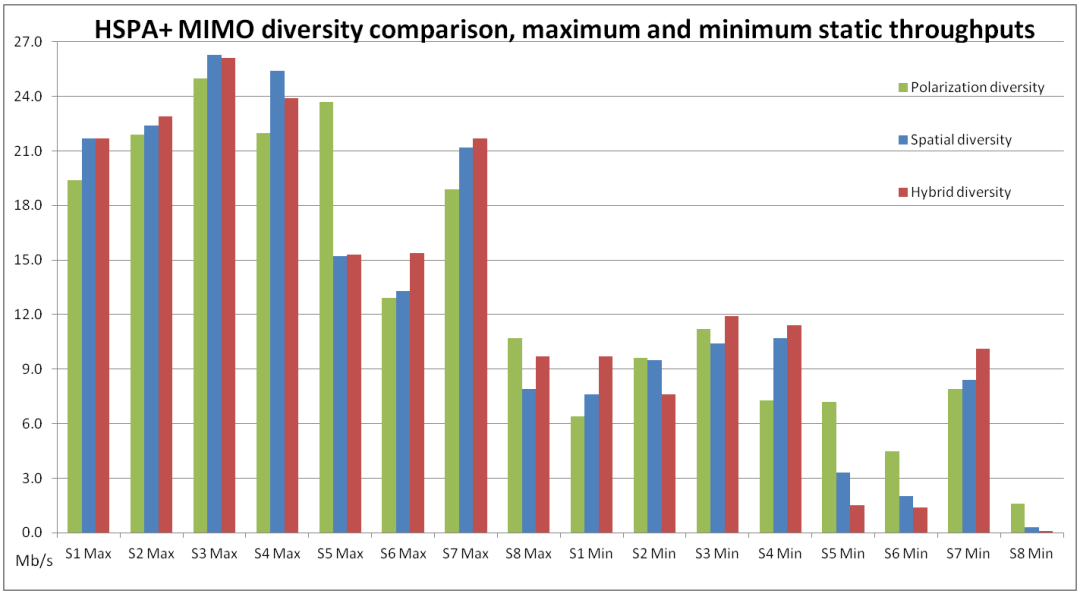

Figure 7.21: *HSPA+ antenna diversity comparison, static results.*

From results presented in figure 7.21, it can be seen that maximum peak rates in every static location, except in spot 5, are close to each other. In spot 5 the polarization diversity appears to achieve much greater peak rate than hybrid or polarization diversity. This indicates that other antenna unit placement can not provide strong MPC propagation to that location, but single antenna unit with polarization diversity can.

With minimum rates for each static location, the results suggest that areas with better channel quality perform alike but spots 5, 6 and 8 with weaker reception are getting better minimum rates with polarization diversity than hybrid or spatial diversity case. Like in mobile section measurements, some of static locations with worse channel quality seem to get better rates with polarization diversity setup. Further analysis of secondary antenna placement would be required to find exact cause and effect for this.

Based on minimum and maximum results in both mobile and static measurements every setup has big variations between minimum and maximum throughput rate, implying that MIMO reception is sensitive and greatly depending of receiver orientation. The constant movement in mobile measurement allows to see similar maximum and minimum rates as static measurements, even though the UE receiver orientation is fixed in mobile measurement cart.

Figure 7.22 shows LTE average throughput rates with each antenna diversity setup. With average results, the performance differences between diversity setups are small similar to case with HSPA+. No setup appears to have notably higher average rates on any mobile section. Only the section 9 in second floor indicates that hybrid diversity achieves notably better rates. The section 9 is short section with only little mobility, consisting of opening and moving through doorway and waiting the door to close. This makes the section 9 results overall little more unpredictable than other mobile sections. From sections 2 and 3 it can be determined that spatial diversity is performing little bit worse on LOS

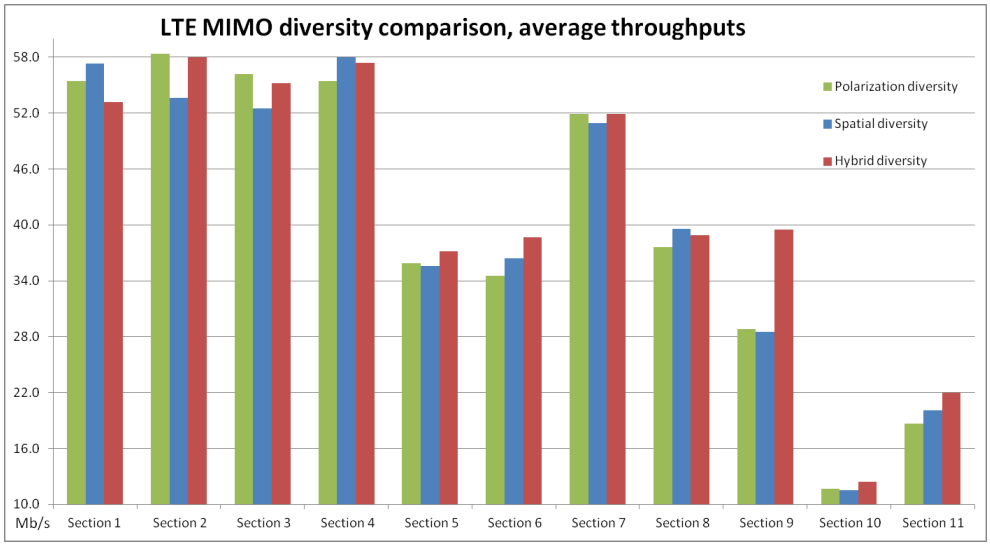

Figure 7.22: *LTE antenna diversity comparison, average results.*

connection than cases with hybrid and polarization diversity.

LTE antenna diversity comparison maximum results are shown in figure 7.23, and minimum results are presented in figure 7.24.

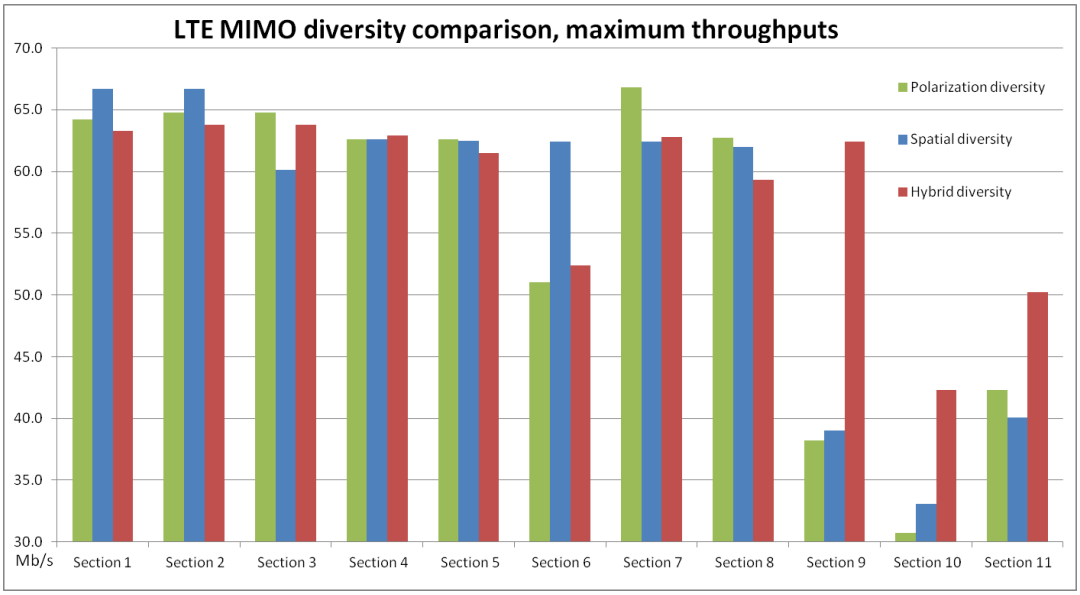

Figure 7.23: *LTE antenna diversity comparison, maximum results.*

Maximum results in first floor section show that maximum peak rates for each diversity case are close to each other. Only in section 6, the spatial diversity scheme achieved notably higher peak rate. Unlike the first floor case where results were even, the second floor sections 9, 10 and 11 clearly indicate that hybrid diversity setup can achieve much greater peak rates than other two cases. Based on results, it is clear that on poor channel condition, the hybrid diversity SM MIMO achieves best peak rates with LTE.

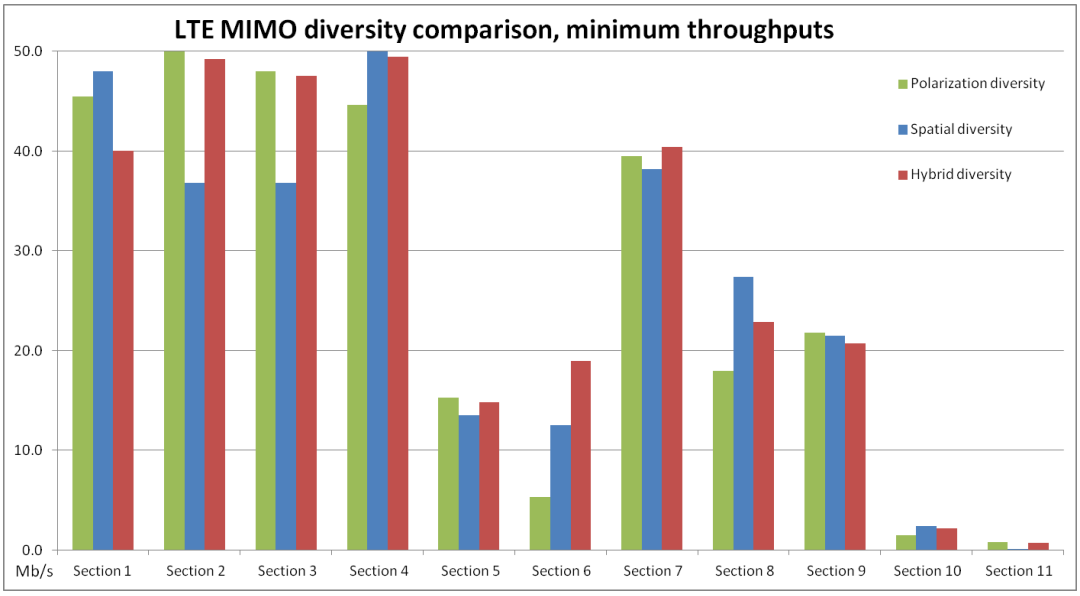

Figure 7.24: *LTE antenna diversity comparison, minimum results.*

The minimum rate results in figure 7.24 indicate that on LOS case in section 2 and 3, the spatial diversity is not performing as well as polarization and hybrid cases. Unlike the maximum throughput rates, the second floor minimum rates do not show dominance with hybrid diversity anymore. In second floor sections, only the section 8 has some difference in minimum rates, favoring spatial diversity and having poorest rate with polarization diversity setup. Overall, the minimum throughput rate differences are not constantly better or worse for any setup.

Static measurement results for antenna diversity setups is shown in figure 7.25. Based

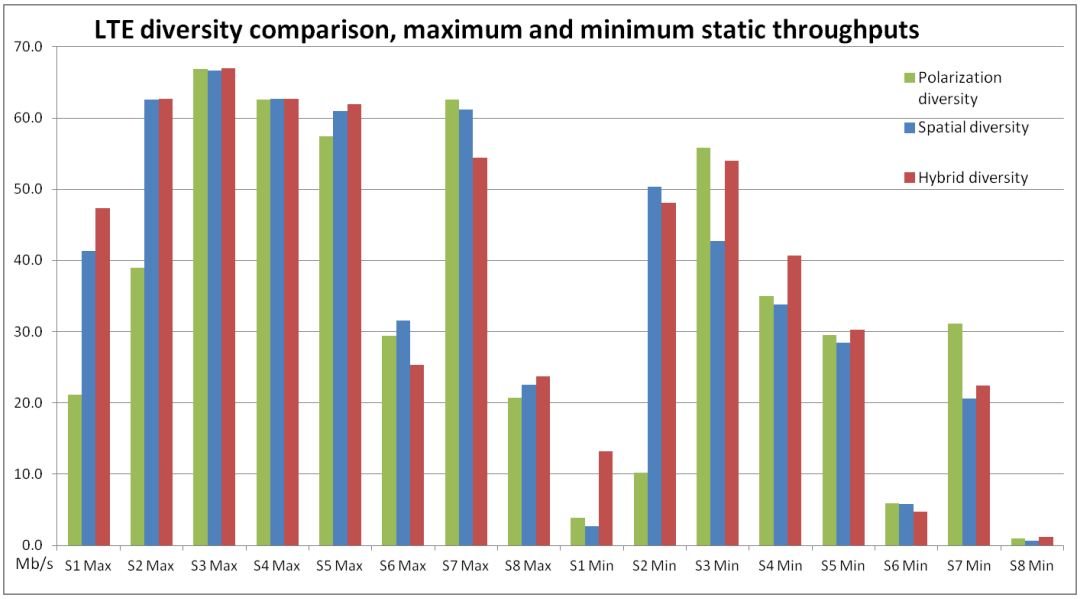

Figure 7.25: *LTE antenna diversity comparison, static results.*

on static results, on the first two static locations both locating behind the antenna unit, polarization diversity rates are considerably lower than spatial or hybrid diversity results. The interference levels and SNR in these static locations were similar for all measurement cases, but MCS values with spatial and hybrid diversity were constantly higher. This result is not seen in HSPA+ case, which indicates that spatial diversity brings notable gain on propagation of LTE signal behind the antenna unit. For other locations, the differences in static throughput rates are not so notable. The difference between maximum and minimum rates are quite high, like in the case with HSPA+.

The LTE SM MIMO is also sensitive to small variations of channel and the orientation of UE receiver. No clear dominance or subpar performance seen in LTE setup when comparing results between diversity setups. Based on all the results, the hybrid diversity seems to have slight edge over other two. On average, the hybrid diversity setup is having most maximum throughputs and has least amount of lowest performances results.

7.4 Antenna line attenuation imbalance effects

This section studies the result of different attenuation levels on MIMO antenna lines. The setup uses reference MIMO configuration with variable attenuator connected to other antenna line. Variable attenuator accuracy was tested and deemed sufficient by using single antenna line setup and measuring RSCP and RSRP values in real time, when increasing and decreasing the attenuation.

Results are divided between first floor and second floor measurements, because first floor MIMO works with higher attenuation levels than second floor. Both HSPA+ and LTE setups work similarly with different attenuation levels. First floor throughput rate begins to drop after about 6dB line difference and MIMO second stream utilization works in first floor up to approximately 13 to 15dB attenuation, after that the SM MIMO did not work. For the second floor, noticeable effect begins already with 3dB attenuation difference, and when attenuation goes over 6dB, dual stream MIMO scheme is not working anymore in second floor.

The increased attenuation for second antenna line had no notable effect on Ec/No and RSRQ levels, but CQI values for second stream degraded as attenuation increased. This caused smaller transmit blocks to be used for second data streams and lower utilization percentage of SM MIMO second data stream. Also the block error rate was higher, causing more re-transmissions in case of higher attenuations. At locations with better channel quality, the effect of attenuation difference seen in throughput is lesser, and on poor channel quality locations the effect on throughput rates is higher.

Figure 7.26 illustrates the throughput rates of HSPA+ first floor antenna attenuation measurements. The throughput graph clearly shows that each measurement case works almost identically along the mobile sections. The throughput rates drop gradually as the attenuation increases. The reference levels is above the attenuation rates almost all the time, and then the lines averages arrange based on the amount of attenuation. The effect

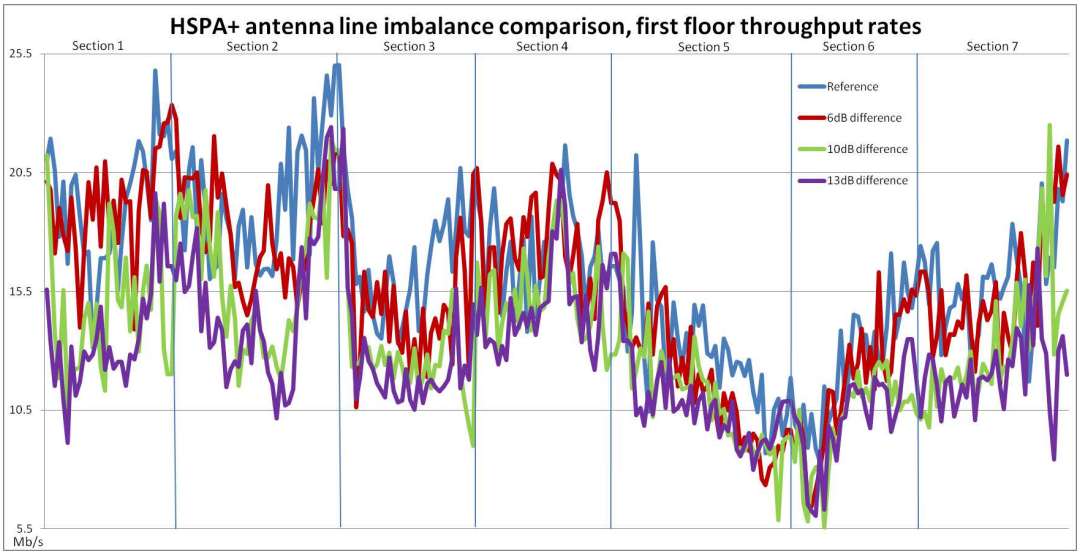

Figure 7.26: *Antenna line attenuation first floor results with HSPA+.*

of increasing attenuation appears to have almost linear effect of average throughput drop.

Calculated from first floor results, the 6dB attenuation difference had 0.83 Mb/s lower average throughput compared to reference case. With 10dB attenuation, the throughput is on average 2.99 Mb/s lower than reference, and 13dB attenuation had 3.67 Mb/s lower throughput on average. Total impact in average throughputs are 5%, 18.2% and 22.4% drop from reference, based on attenuation level.

Figure 7.27 shows the throughput rates of HSPA+ second floor antenna attenuation measurements. Second floor throughput behavior is similar to first floor case, where in-

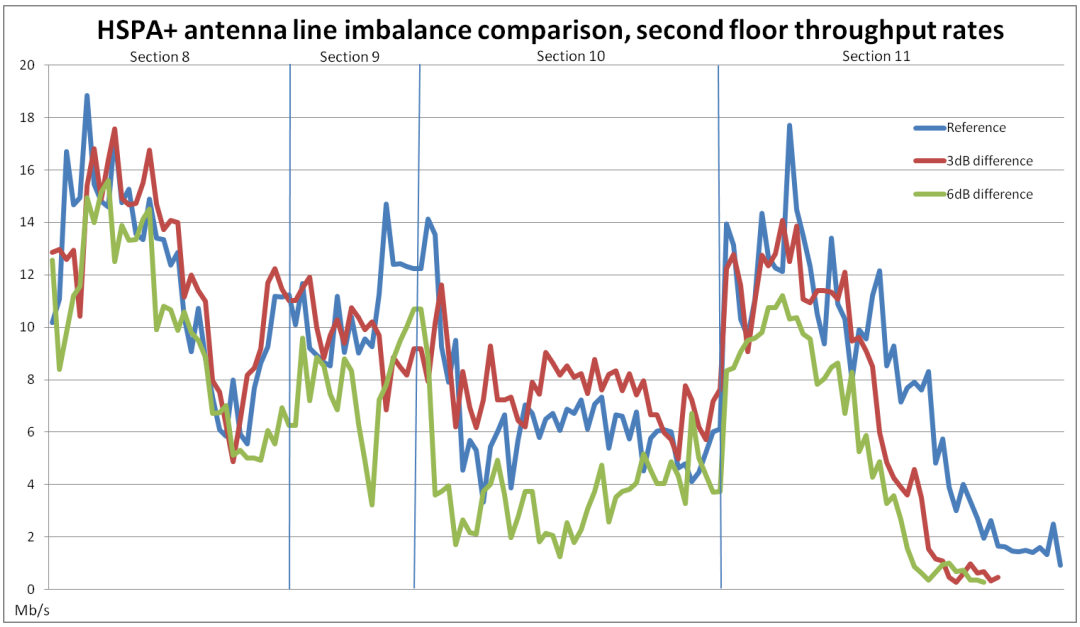

Figure 7.27: *Antenna line attenuation second floor results with HSPA+.*

creased attenuation shows as decreased throughput. Only in section 10, the 3dB line difference seems to outperform reference rate, but this section has low MIMO usage percentage in all measurements, which accounts reference result not providing improvement over small line attenuation case. At the end of section 11 in second floor, it can be seen that with increased attenuation, the cell drop is experienced sooner. Reference measurement could continue few seconds longer than measurements with attenuation along the last route.

From second floor results, the differences in rates are small, but the trend is clearly visible. On average the 3dB attenuation throughput rate is 0.48 Mb/s lower than reference case, causing on average 5% loss in throughput. 6dB attenuation is having 2.4 Mb/s less average throughput compared to reference results, meaning 26.2% drop in average throughput rate.

Figure 7.28 illustrates the throughput rates with LTE first floor antenna attenuation measurements. The results of antenna line imbalance with LTE measurement are very

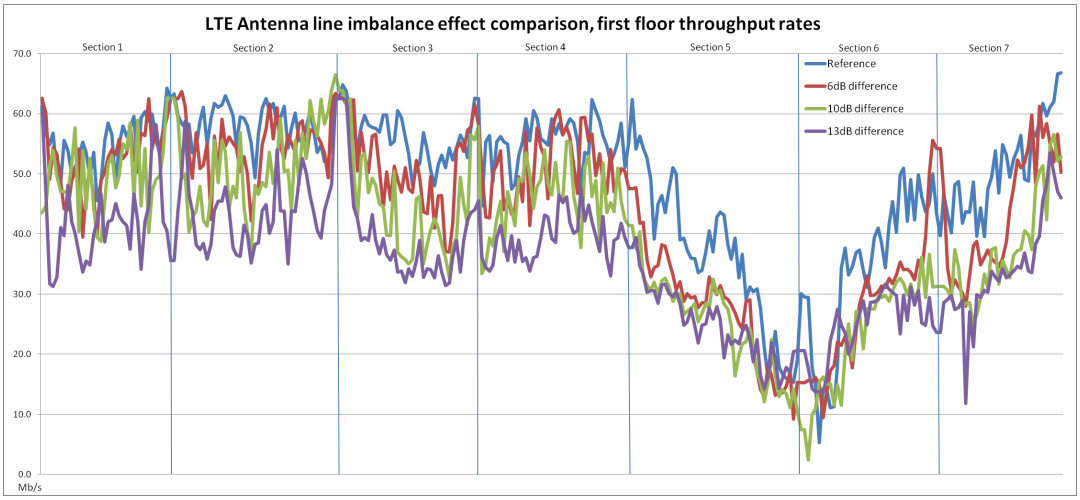

Figure 7.28: *Antenna line attenuation first floor results with LTE.*

much similar as HSPA+ results. The increased attenuation has clear linear drop in the measured throughput rate.

Calculated from first floor results, the 6dB line antenna difference is performing on average 5.51 Mb/s lower than reference case. 10dB difference has on average 9.94 Mb/s lower throughput rate in first floor than reference case. And 13dB antenna line attenuation performs at 14.33 Mb/s lower average rate. These account for 11%, 20% and 28.9% decrease in average throughput rate.

Figure 7.29 presents the throughput rates with LTE second floor antenna attenuation measurements. Also the second floor throughput behavior with different attenuation levels is behaving as expected and seen in HSPA+ case. Only few crossing of throughput lines happen, mostly during bad sections for MIMO utilization. Also its noticeable that the cell drop, experienced at the end of section 11, happens sooner with cases of more attenuation. It is apparent that diversity gain from two antenna lines can provide small extend to the

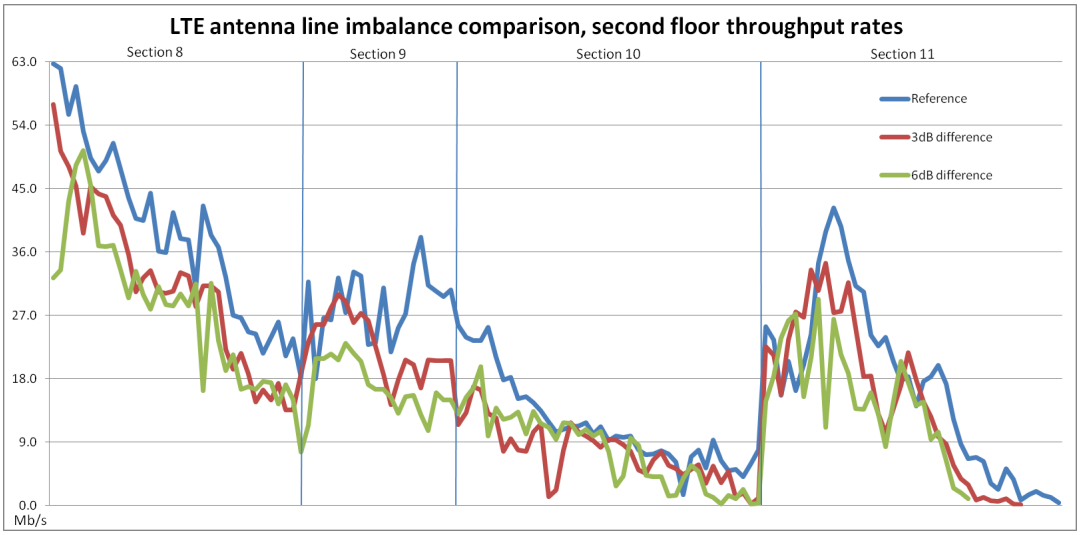

Figure 7.29: *Antenna line attenuation second floor results with LTE.*

reception area at the edge of the cell.

Based on second floor results, 3dB attenuation difference has on average 4.8 Mb/s lower throughput rate, corresponding to 19.6% decrease in performance. With 6dB attenuation difference the impact is 7.3 Mb/s lower average throughput rate, having 30.2% decrease in performance experienced in second floor.

8. DISCUSSION AND CONCLUSIONS

From theoretical point of view, the spatial multiplexing scheme in wireless mobile networks is performing best in good coverage areas with strong signal levels and good multipath propagation. The indoor environment in this sense is offering suitable basis for experiencing best gains in performance and capacity utilization MIMO can offer. In concept, the idea of using multiple antennas in wireless communication has been around for almost two of decades, but actual implementations for SM related capacity gain has only been implemented very recently in cellular networks. Only the latest evolution of 3G WCDMA and the new next generation LTE network implement the SM MIMO functionality for capacity and performance gain.

The test measurements performed in a small indoor cell, studied the performance of MIMO scheme with various different setups. Based on results, it can be seen that MIMO setup can provide notable gain over traditional single antenna setups. It is also notable that best performance improvement seen with SM happens in good channel conditions, with LOS or close proximity with antenna On average the good channel conditions give about 50% to 60% increase in throughput compared to single line wiht single data stream.

When the distance or amount of big obstacles, like walls or doors, between transmitter and receiver increases, the channel quality decreases affecting SM MIMO performance more than single data stream transmission. On these worse channel conditions, the utilization percentage of dual stream is low, and average throughput gain spatial multiplexing scheme can provide against single antenna setup is ranging from 5% to 30%.

When studying same test cases with both HSPA+ and LTE setups, it can also be concluded that OFDMA digital modulation scheme used by the LTE is more suitable with MIMO setup than WCDMA. The throughput variations with HSPA+ are faster and proportionately larger than with LTE. Although it has to be taken to consideration that the time of the measurements were performed, LTE only had few commercially available USB modems and HSPA+ had only the single modem capable of UE category 18 support, and it had to be firmware updated to support MIMO. In the future, there is likely going to be more MIMO supporting HSPA+ modems and other UEs, that might have better reception and more stable performance. LTE is certainly going to evolve and have many various types of terminals and UEs in near future. In this sense, the MIMO performance and gain can most likely be increased over time with maturing technology.

There were some notable observations during measurements and result analysis based on MIMO performance. The HSPA+ setup throughput performance follows closely to received pilot signal power behavior, suggesting that with HSPA+ the MIMO performance

gradually drops as the distance to BTS transmit antenna increases. The effect of multipath propagation changes was not so obvious with HSPA+. With LTE, the effect was different. With good reference signal levels, the throughput kept constantly high and did not follow the RSRP rate. Instead, the propagation environment effect was notable, when moving behind corners and more obstacles, the RSRP levels did not drop as much as the MIMO throughput rate. The behavior of LTE MIMO performance on good coverage areas is more dependent on channel conditions for two data stream propagation.

The static measurements gave good insight of how sensitive SM MIMO reception is. The effect of receiver orientation has great impact on the throughput rates experienced in a fixed static spot. This implies that the small distance and some type of polarization or antenna directivity pattern difference between receiver antennas of USB modem are highly sensitive to signal propagation direction in downlink. Even few degree rotation can cause over 50% drop in experienced throughput. This effect is not very visible in mobile measurements, where constant movement helps to give a small variation to channel and prevent fast and big variances in throughputs. Altough it can be seen from results, that crossing between mobile measurement section show rise in throughput rate. This is caused by short stop in order to place a marker comment in measurement log. The increase in throughput rates during stops suggest that the mobility has small negative effect on maximum peak rates.

Comparison of different antenna diversity setups gave expected results. All the different ways to provide diversity required to use SM MIMO provided similar performance. Throughput differences were small and varied between test sections and spots. Overall, the hybrid diversity setup can be considered best on average by small difference, and spatial diversity seem to perform worst on LOS sections. The easiest installation comes with polarization diversity, where one antenna unit is enough, because no spatial distance between antenna elements is needed. Results were similar for both HSPA+ and LTE except a few minor differences in some cases.

Also, antenna feeder line imbalance measurement results were consistent with expectations. For both HSPA+ and LTE, antenna line imbalance setup performed close to a linear case, where increased attenuation to other antenna line directly shows as decreased throughput. Sections with better channel quality have lesser impact from attenuation, and when channel quality degrades, the decrease in throughput becomes larger.

On first floor measurements, the imbalance level started to show difference around 5 to 6dB attenuation difference, and second data stream utilization still worked properly with up to 13 - 15dB attenuation difference. In second floor case, smaller attenuation difference already showed same linear effects as in first floor. Greater than 6dB attenuation prevented SM MIMO from working in the second floor, resulting performance similar to single antenna line case. It can be concluded from these results that MIMO performance is affected by antenna line imbalance, but it is not sensitive to very small imbalance levels.

Overall these results and studies appear to be consistent with MIMO theory and mea-

sured throughput levels and parameters were, for the most parts, as expected. Aim for these results is to give better understanding of MIMO scheme gain and performance in indoor environment, and give estimates and information about expected gains network operators can consider when planning indoor networks.

For further analysis points, there would ideally be test cases with interference from other networks and neighboring cells, and more users causing interference and load to the cells and core network. Also studying the MIMO performance in a larger DAS indoor network where multiple antennas are utilized to provide a coverage for MIMO cell. And a study of MIMO gain in uplink direction obtained by receiver diversity would be interesting case. In addition, the required distance between antenna elements for providing sufficient spatial diversity for indoor SM MIMO could provide an additional measurement topic.

BIBLIOGRAPHY

[1] H. Holma & A. Toskala, "LTE for UMTS OFDMA and SC-FDMA Based Radio Access", John Wiley & Sons Ltd., 2009

[2] Karl J. Molnar & Stephen J. Grant, "Performance of Dedicated Indoor MIMO HS-DPA Systems", Article in Vehicular Technology Conference, VTC 2008-Fall. IEEE 68th, 2008

[3] Xiao Peng Yang, Qiang Chen & Kunio Sawaya, "Effect of Antenna Locations on Indoor MIMO System", IEEE Antennas and Wireless Propagation Letters, Vol. 6, 2007

[4] Jishu DasGupta, Karla Ziri-Castro & Hajime Suzuki, "Capacity Analysis of MIMO-OFDM Broadband Channels In Populated Indoor Environments", Communications and Information Technologies, 2007. ISCIT ’07. International Symposium, 2007

[5] A. Paulraj & T. Kailath, US Patent No. 5345599 on Spatial Multiplexing, issued 1994

[6] Gregory G. Raleigh & John M. Cioffi, "Spatio-temporal coding for wireless communication", IEEE Transactions on Communications, Vol. 46, No. 3, pp. 357-366, March 1998

[7] Gerald J. Foschini, "Layered space-time architecture for wireless communication in a fading environment when using multiple antennas", Bell Labs Syst. Technical Journal, Vol. 1, pp. 41-59, Autumn 1996

[8] G. D. Golden, G. J. Foschini, R. A. Valenzuela, & P. W. Wolniansky, "Detection algorithm and initial laboratory results using V-BLAST space-time communication architecture", Electronic Letter, Vol. 35, pp. 14-16, January 1999

[9] "MIMO Formats - SISO, SIMO, MISO, MU-MIMO", [WWW], [Referred 22.6.2011], Available: http://www.radio-electronics.com/info/antennas/mimo/formats-siso-simo-miso-mimo.php

[10] C.E. Shannon, "A Mathematical Theory of Communication", Bell System Technical Journal, Vol. 27, pp. 379-423, 623-656, July and October 1948

[11] E. Dahlman, S. Parkvall, J. Sköld & P. Beming, "3G Evolution HSPA and LTE for Mobile Broadband", Second edition, Elsevier Ltd., 2008

[12] Telmo André Rodrigues Batista, "Capacity increase in UMTS/HSPA+ Through the Use of MIMO Systems", Master of Science Thesis, Instituto Superior Técnico (IST), Portugal, July 2008

[13] P. Almers, F. Tufvesson, O. Endfors & A. Molisch, "Measured Capacity gain using waterfilling in frequency selective MIMO channels", 13th IEE International Symposion on Personal, Indoor and Mobile Radio Communications, September 2002

[14] D. P. Palomar & J. R. Fonolloza, "Practical Algorithms for a Family of Waterfilling Solutions", IEEE Transactions of Signal Processing, Vol. 53, No. 2, February 2005

[15] Vikram R. Anreddy, "Indoor MIMO Channels with Polarization Diversity: Measurements and Performance Analysis", Master of Science Thesis, School of Electrical and Computer Engineering Georgia Institute of Technology, May 2006

[16] K. Raoof, M. Ben Zid, N. Prayongpun & A. Bouallegue, "Advanced MIMO Techniques: Polarization Diversity and Antenna Selection", InTech, April 2011

[17] J. J. A. Lempiäinen & J. K. Laiho-Steffens, "The Performance of Polarization Diversity Schemes at a Base Station in Small/Micro Cells at 1800 MHz", IEEE Transaction on Vehicular Technology, Vol. 47, No. 3, August 1998

[18] J. Wang, Z. Zhang & Y. Gong, WA Comparison of Reception Schemes for Interference Suppression in MIMO-OSTBCs System", Communications, Circuits and Systems, ICCCAS International Conference, July 2009

[19] C. Wang, Edward K. S., R. D. Murch, W. H. Mow, R. S. Cheng & V. Lau, "On the Performance of the MIMO Zero-Forcing Receiver on the Presence of Channel Estimation Error", IEEE Transactions on Wireless Communications, Vol. 6, No. 3, March 2007

[20] Y. Jiang, M. K. Varanasi, J. Li, "Performance Analysis of ZF and MMSE Equalizers for MIMO Systems: An In-Depth Study of the High SNR Regime, University of Colorado, presented in part at Globecom, 2005

[21] Karen Su, "Efficient Maximum Likelihood detection for communication over Multiple Input Multiple Output channels", report in part of research for PhD degree, University of Cambridge, February 2005

[22] S. Grant et al., "Per-Antenna-Rate-Control (PARC) in Frequency Selective Fading with SIC-GRAKE Receiver", 60th IEEE Vehicular Technology Conference, Vol. 2, pp. 1458-1462, September 2004

[23] A. Burg, M.Wenk, M. Zellweger, W. Fichtner, & H. Bolcskei, "VLSI Implementation of MIMO Detection Using the Sphere Decoding Algorithms", IEEE Journal of Solid-State Circuits, Vol. 40, No. 7, pp. 1566-1576, July 2005.

[24] Q. Li & Z. Wang, "New Sphere Decoding Architecture for MIMO Systems", School of EECE, Oregon State University

[25] S. Caban, C. MehlfÄuhrer, A. L. Scholtz, & M. Rupp, "Indoor MIMO Transmissions with Alamouti Space -Time Block Codes", Research publication 2005, Vienna University of Technology

[26] Lekun Lin, PhD, "Choosing between open- and closed-loop MIMO in BTS systems" Article in Embedded Computing Design, May 15th 2009

[27] R.W. Heat, Jr. & A. J. Paularj, "Switching between diversity and multiplexing in MIMO systems", IEEE Transactions on Communications, Vol. 53, No. 6, pp. 962-968, June 2005

[28] Haroon Shan, "Comparison of picocell and DAS configuration with HSPA Evolution", Master of Science Thesis, Tampere University of Technology (TUT), Finland, March 2011

[29] Editor: J-P. M. G. Linnartz, Co-author: J. S. Davis, "Wireless Communication - Indoor Wireless RF Channels" [WWW] [Referred 18.7.2011], Available: http://wireless.per.nl/reference/chaptr03/indoor.htm & http://wireless.per.nl/reference/chaptr03/ricepdf/rice.htm

[30] X. P. Yang, Q. Chen & K. Sawaya, "Effect of Antenna Locations on Indoor MIMO Systems", IEEE Antennas and Wireless Propagation Letters, Vol. 6, 2007

[31] Minfei Leng, "How to Properly Design an In-Building Distributed Antenna System", Technical Article by Bird Technologies Group

[32] J. Bergman, D. Gerstenberger, F. Gunnarsson & S. Ström, "Continued HSPA Evolution of mobile broadband", Ericsson Review, 1/2009

[33] Chris Johnson, "Radio access networks for UMTS", John Wiley & Sons Ltd, 2008

[34] Motorola, "Overview of LTE Air-Interface", Technical White Paper, 2007

[35] ATDI "Mobile LTE Network design with ICS telecom", White Paper, December 2008

[36] Dongzhe Cui, "LTE Peak Rates Analysis", Wireless and Optical Communications Conference, November 2009

[37] 3GPP TS 36.213; "Technical Specification Group Radio Access Network; Evolved Universal Terrestrial Radio Access (E-UTRA); Physical layer procedures (Release 8)", Version 8.8.0 (2009-09).

[38] 3GPP TS 25.212; "Multiplexing and Channel Coding (FDD), Release 8", Version 8.6.0 (2009-09).

APPENDIX A

Appendix A lists all throughput values gathered from measurement results in a table format. Each table contains field for maximum, minimum, average and standard deviation values for each section or static spot, given in megabyte per second (Mb/s). Maximum and minimum values represent maximum and minimum values measured on section or static spot. Average value is averaged throughput rate in a section or a spot, and standard deviation indicates how big variation the throughput values have over measurement area. Small standard deviation means that throughput rate changes are small and big standard deviation implies that variations in throughput rates are large. Standard deviation is defined as square root of variance, while variance is defined as average squared differences of average data values in a set.

Reference SM MIMO results

Table 1 presents the mobile results of HSPA+ with reference MIMO setup.

Table 1: *HSPA+ reference mobile throughput results.*

Section	1	2	3	4	5	6	7	8	9	10	11
Max	24.7	25.0	25.0	21.6	21.2	17.4	21.9	18.8	14.7	14.1	17.7
Min	13.1	16.4	13.3	13.7	8.4	8.3	11.7	3.4	8.0	3.3	0.9
Avg	19.6	20.1	16.9	17.0	12.8	12.6	15.8	10.7	11.2	7.1	7.7
StDev	2.4	2.2	2.7	2.1	2.6	2.3	2.6	3.5	2.0	2.0	4.4

Table 2 presents the static results of HSPA+ with reference MIMO setup.

Table 2: *HSPA+ reference static measurement throughput results.*

Spot	1	2	3	4	5	6	7	8
Max	19.4	21.9	25.0	22.0	23.7	12.9	18.9	10.7
Min	6.4	9.6	11.2	7.3	7.2	4.5	7.9	1.6
Avg	11.5	16.0	20.3	15.4	16.0	9.2	13.6	6.0
StDev	2.9	4.0	3.1	3.7	3.3	2.2	2.5	2.2

Table 3 presents the mobile results of LTE with reference MIMO setup.

Table 3: *LTE reference mobile throughput results.*

Section	1	2	3	4	5	6	7	8	9	10	11
Max	64.2	64.8	64.8	62.6	62.6	51.0	66.8	62.7	38.2	30.7	42.3
Min	45.5	52.0	48.0	44.6	15.3	5.3	39.5	18.0	21.8	1.5	0.8
Avg	55.4	58.4	56.2	55.4	35.9	34.5	51.9	37.6	28.8	11.7	18.7
StDev	5.4	3.3	4.1	4.9	12.4	12.8	8.4	11.5	5.7	6.2	12.2

Table 4 presents the static results of LTE with reference MIMO setup.

Table 4: *LTE reference static measurement throughput results.*

Spot	1	2	3	4	5	6	7	8
Max	21.2	39.0	66.9	62.6	57.4	29.4	62.5	20.7
Min	3.8	10.2	55.8	35.0	29.5	5.9	31.2	1.0
Avg	15.0	26.3	62.7	51.6	44.6	19.0	45.5	10.7
StDev	4.0	8.8	2.4	7.5	7.7	5.0	7.2	6.2

MIMO gain results

Table 5 presents the results for HSPA+ single antenna line with 16-QAM modulation configuration.

Table 5: *HSPA+ single antenna line with 16-QAM results.*

Section	1	2	3	4	5	6	7	8	9	10	11
Max	13.5	13.5	13.5	13.5	13.3	13.5	13.5	12.5	12.0	11.0	12.1
Min	12.4	12.5	11.0	11.4	6.6	7.1	10.4	5.8	7.5	4.4	0.2
Avg	13.2	13.2	12.0	13.0	10.9	11.0	12.5	9.8	9.9	6.8	6.7
StDev	0.3	0.2	0.7	0.4	1.6	1.9	0.7	2.1	1.4	1.5	4.4

Table 6 presents the results for HSPA+ transmit diversity MIMO with 16-QAM modulation configuration.

Table 6: *HSPA+ transmit diversity MIMO with 16-QAM results.*

Section	1	2	3	4	5	6	7	8	9	10	11
Max	13.5	13.5	13.5	13.5	13.5	13.2	13.5	12.8	13.4	12.4	12.4
Min	12.6	12.9	10.9	12.2	7.7	7.8	11.7	6.2	9.1	5.1	0.7
Avg	13.3	13.3	12.3	13.0	11.3	11.1	12.1	10.7	11.3	9.1	6.9
StDev	0.2	0.1	0.8	0.3	1.7	1.6	0.6	1.8	1.1	1.6	4.6

Table 7 presents the results for HSPA+ single antenna line with 64-QAM modulation configuration.

Table 7: *HSPA single antenna line with 64-QAM results.*

Section	1	2	3	4	5	6	7	8	9	10	11
Max	19.5	19.7	18.9	18.6	17.2	17.4	19.3	15.8	8.7	8.1	11.9
Min	15.9	15.4	11.6	14.5	7.3	5.9	12.4	3.8	5.7	1.3	0.7
Avg	17.6	17.1	15.2	16.7	12.5	12.1	15.3	10.0	6.6	5.2	5.7
StDev	0.8	0.6	1.8	0.9	2.8	3.2	1.8	3.9	1.2	1.2	3.6

Table 8 presents results for HSPA+ transmit diversity MIMO with 64-QAM modulation configuration.

Table 8: *HSPA transmit diversity MIMO with 64-QAM results.*

Section	1	2	3	4	5	6	7	8	9	10	11
Max	20.0	19.1	18.2	19.1	17.9	17.9	19.5	16.3	15.6	13.3	13.6
Min	16.2	16.2	12.9	15.2	6.9	7.6	13.0	7.1	10.2	3.2	0.4
Avg	17.3	17.5	15.1	17.0	12.9	12.8	15.7	12.0	13.1	8.3	7.4
StDev	1.1	0.6	1.5	0.8	3.0	3.3	1.8	2.8	1.5	2.0	5.0

Table 9 presents results for LTE single antenna line configuration.

Table 9: *LTE single antenna line results.*

Section	1	2	3	4	5	6	7	8	9	10	11
Max	35.7	35.7	35.7	35.8	35.7	34.8	35.7	35.5	22.1	20.6	27.1
Min	35.5	34.9	33.1	35.3	4.5	8.3	26.4	15.0	14.0	0.1	0.3
Avg	35.7	35.6	35.2	35.6	24.3	25.0	33.1	24.2	17.8	7.3	14.4
StDev	0.1	0.1	0.6	0.1	9.0	7.0	2.9	6.7	2.4	5.8	8.3

Table 10 presents results for LTE transmit diversity MIMO configuration.

Table 10: *LTE transmit diversity MIMO results.*

Section	1	2	3	4	5	6	7	8	9	10	11
Max	33.6	33.6	33.6	33.6	33.6	32.9	33.7	33.6	28.2	28.0	31.1
Min	33.4	33.3	33.0	33.1	14.7	15.9	30.8	12.4	13.7	0.7	0.1
Avg	33.6	33.5	33.4	33.5	27.9	28.2	32.7	29.4	21.6	11.8	23.0
StDev	0.1	0.1	0.2	0.1	5.7	5.8	0.9	4.8	4.3	6.3	8.2

SM MIMO Antenna diversity setup comparison

Table 11 presents mobile results for HSPA+ spatial diversity setup.

Table 11: *HSPA+ spatial diversity mobile results.*

Section	1	2	3	4	5	6	7	8	9	10	11
Max	23.5	22.1	22.0	22.3	19.9	21.9	25.1	18.3	11.7	10.9	15.4
Min	16.6	11.5	12.2	14.6	8.4	7.5	12.7	5.0	7.0	2.0	0.4
Avg	19.4	17.2	16.3	17.7	13.7	13.8	17.0	11.7	10.1	4.3	8.2
StDev	1.9	2.7	2.6	1.5	2.8	3.4	3.0	3.7	1.3	1.7	4.7

Table 12 presents static results for HSPA+ spatial diversity setup.

Table 12: *HSPA spatial diversity static results.*

Spot	1	2	3	4	5	6	7	8
Max	21.7	22.4	26.3	25.4	15.2	13.3	21.2	7.9
Min	7.6	9.5	10.4	10.7	3.3	2.0	8.4	0.3
Avg	14.4	15.6	19.6	17.6	9.4	8.8	15.0	3.7
StDev	3.5	3.5	3.5	3.6	2.9	2.2	3.6	2.0

Table 13 presents mobile results for HSPA+ hybrid diversity setup.

Table 13: *HSPA+ hybrid diversity mobile results.*

Section	1	2	3	4	5	6	7	8	9	10	11
Max	24.9	26.1	25.5	21.4	21.7	21.9	23.6	18.9	12.9	8.7	15.2
Min	15.4	14.1	13.4	15.5	9.0	4.8	13.2	6.1	8.0	2.0	1.7
Avg	19.6	18.8	17.5	18.6	14.0	13.9	17.8	12.6	9.8	4.5	8.1
StDev	2.2	2.4	2.8	1.6	3.0	3.2	2.8	3.8	1.3	1.6	4.4

Table 14 presents static results for HSPA+ hybrid diversity setup.

Table 14: *HSPA+ hybrid diversity static results.*

Spot	1	2	3	4	5	6	7	8
Max	21.7	22.9	26.1	23.9	15.3	15.4	21.7	9.7
Min	9.7	7.6	11.9	11.4	1.5	1.4	10.1	0.1
Avg	13.5	15.8	21.1	17.9	8.3	9.8	15.3	4.9
StDev	3.1	3.6	2.9	3.3	2.7	3.3	2.9	2.2

Table 15 presents mobile results for HSPA+ spatial diversity setup.

Table 15: *LTE spatial diversity mobile results.*

Section	1	2	3	4	5	6	7	8	9	10	11
Max	66.7	66.7	60.1	62.6	62.5	62.4	62.4	62.0	39.0	33.1	40.1
Min	48.0	36.8	36.8	51.9	13.5	12.5	38.2	27.4	21.5	2.4	0.1
Avg	57.3	53.6	52.5	58.0	35.6	36.4	50.9	39.6	28.5	11.5	20.1
StDev	4.5	7.4	5.3	2.9	13.9	14.1	7.5	9.9	5.6	7.0	11.4

Table 16 presents static results for HSPA+ spatial diversity setup.

Table 16: *LTE spatial diversity static results.*

Spot	1	2	3	4	5	6	7	8
Max	41.3	62.6	66.7	62.7	61.0	31.6	61.2	22.5
Min	2.7	50.3	42.7	33.8	28.4	5.8	20.6	0.7
Avg	24.5	58.7	60.1	53.6	44.5	15.7	41.9	12.9
StDev	7.7	3.4	5.1	6.6	8.0	6.5	8.7	5.6

Table 17 presents mobile results for HSPA+ hybrid diversity setup.

Table 17: *LTE hybrid diversity mobile results.*

Section	1	2	3	4	5	6	7	8	9	10	11
Max	63.3	63.8	63.8	62.9	61.5	52.4	62.8	59.3	62.4	42.3	50.2
Min	40.0	49.3	47.5	49.4	14.8	19.0	40.4	22.9	20.7	2.2	0.7
Avg	53.2	58.0	55.2	57.4	37.2	38.7	51.9	38.9	39.5	12.4	22.0
StDev	6.8	3.9	5.0	3.2	12.2	10.3	6.1	9.8	11.2	8.3	14.0

Table 18 presents static results for HSPA+ hybrid diversity setup.

Table 18: *LTE hybrid diversity static results.*

Spot	1	2	3	4	5	6	7	8
Max	47.3	62.7	67.0	62.7	61.9	25.3	54.4	23.7
Min	13.2	48.0	54.0	40.6	30.3	4.8	22.4	1.2
Avg	30.8	59.5	61.6	51.4	44.7	16.1	41.4	15.8
StDev	7.3	3.6	3.1	7.0	7.4	5.6	7.5	5.0

Antenna line attenuation imbalance effects

Table 19 presents first floor 3dB antenna line attenuation difference results for HSPA+.

Table 19: *HSPA+ first floor 3dB attenuation difference.*

Section	1	2	3	4	5	6	7
Max	21.2	21.9	22.0	22.8	17.5	17.3	22.3
Min	17.1	14.9	11.4	14.0	8.4	6.7	13.6
Avg	18.9	18.7	15.7	17.5	12.7	12.6	16.7
StDev	1.3	2.1	3.4	2.7	2.7	3.1	2.7

Table 20 presents first floor 6dB antenna line attenuation difference results for HSPA+.

Table 20: *HSPA+ first floor 6dB attenuation difference.*

Section	1	2	3	4	5	6	7
Max	22.6	23.4	21.3	20.9	19.2	16.3	21.6
Min	13.9	14.5	10.6	14.0	7.3	6.4	11.6
Avg	19.1	18.3	14.9	17.7	11.8	11.7	15.5
StDev	2.2	2.4	2.5	2.0	2.8	2.8	2.5

Table 21 presents first floor 10dB antenna line attenuation difference results for HSPA+.

Table 21: *HSPA+ first floor 10dB attenuation difference.*

Section	1	2	3	4	5	6	7
Max	21.2	21.9	21.4	19.3	17.1	12.6	22.5
Min	10.5	11.5	9.0	12.2	5.9	5.6	9.8
Avg	14.9	16.1	13.0	15.4	11.1	10.0	13.4
StDev	2.7	2.9	2.5	1.8	2.2	2.0	2.7

Table 22 presents first floor 13dB antenna line attenuation difference results for HSPA+.

Table 22: *HSPA+ first floor 13dB attenuation difference.*

Section	1	2	3	4	5	6	7
Max	19.6	22.4	22.3	20.6	17.1	13.5	17.3
Min	9.1	10.2	10.5	12.2	8.0	6.1	8.4
Avg	13.5	14.9	12.7	14.9	10.7	10.2	12.2
StDev	2.3	3.0	2.6	2.0	1.8	2.0	1.6

Table 23 presents second floor 3dB antenna line attenuation difference results for HSPA+.

Table 23: *HSPA+ second floor 3dB attenuation difference.*

Section	8	9	10	11
Max	17.6	11.9	11.6	14.1
Min	4.9	6.9	5.0	0.3
Avg	12.2	9.7	7.6	7.2
StDev	3.3	1.3	1.2	5.0

Table 24 presents second floor 6dB antenna line attenuation difference results for HSPA+.

Table 24: *HSPA+ second floor 6dB attenuation difference.*

Section	8	9	10	11
Max	15.6	10.7	10.7	11.2
Min	4.9	3.2	1.2	0.3
Avg	9.9	7.8	3.8	5.6
StDev	3.6	1.9	1.9	4.0

Table 25 presents first floor 6dB antenna line attenuation difference results for LTE.

Table 25: *LTE first floor 6dB attenuation difference.*

Section	1	2	3	4	5	6	7
Max	62.6	63.7	62.6	60.7	47.7	55.6	61.2
Min	39.4	42.2	37.0	41.4	9.2	9.5	28.0
Avg	52.7	55.1	50.9	51.1	27.3	28.3	43.7
StDev	5.9	5.3	6.7	5.3	9.5	11.1	10.2

Table 26 presents first floor 10dB antenna line attenuation difference results for LTE.

Table 26: *LTE first floor 10dB attenuation difference.*

Section	1	2	3	4	5	6	7
Max	62.6	66.5	63.9	55.4	41.4	36.6	56.5
Min	38.8	36.9	32.7	33.4	7.4	2.4	25.0
Avg	49.7	51.6	45.0	45.8	24.7	23.9	37.4
StDev	6.3	7.3	8.7	5.5	8.3	8.9	9.4

Table 27 presents first floor 13dB antenna line attenuation difference results for LTE.

Table 27: *LTE first floor 13dB attenuation difference.*

Section	1	2	3	4	5	6	7
Max	61.2	62.5	62.5	47.6	39.4	31.6	53.5
Min	31.3	33.0	14.3	13.6	11.9	13.6	11.9
Avg	42.0	43.9	38.9	39.3	24.8	24.7	33.8
StDev	7.8	7.4	7.9	3.9	6.2	5.6	9.0

Table 28 presents second floor 3dB antenna line attenuation difference results for LTE.

Table 28: *LTE second floor 3dB attenuation difference.*

Section	8	9	10	11
Max	57.0	29.9	24.8	34.4
Min	13.5	14.3	0.2	0.1
Avg	30.3	22.6	9.4	15.5
StDev	11.5	4.8	4.7	11.0

Table 29 presents second floor 6dB antenna line attenuation difference results for LTE.

Table 29: *LTE second floor 6dB attenuation difference.*

Section	8	9	10	11
Max	50.4	23.1	19.7	29.3
Min	7.6	10.6	0.1	1.0
Avg	27.1	17.2	7.9	15.4
StDev	10.3	3.7	5.3	7.6